NASA
Technical
Paper
2190

September 1983

Crash Tests of Three Identical Low-Wing Single-Engine Airplanes

Claude B. Castle
and Emilio Alfaro-Bou

NASA

25th Anniversary
1958-1983

NASA
Technical
Paper
2190

1983

Crash Tests of Three Identical Low-Wing Single-Engine Airplanes

Claude B. Castle
and Emilio Alfaro-Bou
Langley Research Center
Hampton, Virginia

NASA
National Aeronautics
and Space Administration

**Scientific and Technical
Information Branch**

Page Intentionally Left Blank

CONTENTS

SUMMARY

Three identical four-place, low-wing single-engine airplane specimens with nominal masses of 1043 kg were crash-tested at the Langley Impact Dynamics Research Facility under controlled free-flight conditions. The tests were conducted at the same nominal impact velocity of 25 m/sec along the flight path. Two airplane specimens were crashed on a concrete surface (at 10° and -30° pitch angles), and one was crashed on soil (at a -30° pitch angle).

The three tests revealed that the specimen in the -30° test on soil sustained massive structural damage in the engine compartment and fire wall. Severe damage, but of lesser magnitude, occurred in the -30° test on concrete, and the least structural damage was experienced in the 10° test on concrete.

An average longitudinal cabin-floor acceleration of -26g occurred in the -30° test on soil. An average normal cabin-floor acceleration of -29g occurred in the -30° test on concrete. Accelerations in the 10° test on concrete were the lowest for the three tests. In the -30° test on soil, the longitudinal acceleration on the pilot's pelvis was -60g; whereas for the -30° test on concrete, the acceleration was -23g. The tensions in the pilot's lap belt for the two -30° tests was 3700 N and 200 N, respectively. The normal acceleration in the pilot's seat pan was -8g and -37g, respectively. The 10° test on concrete produced a longitudinal pelvis acceleration of -6g, negligible lap-belt tension, and a normal seat-pan acceleration of -14g.

INTRODUCTION

With the rapid growth of private and commercial air traffic since World War II, increasing emphasis has been focused on the causes of passenger injuries and death in severe, but potentially survivable, crashes. The National Advisory Committee for Aeronautics (NACA) conducted a series of full-scale airplane crash tests with instrumented dummies in the 1950's. (See refs. 1 and 2.) These tests were performed by accelerating the airplane along a horizontal guide rail and crashing it into an earthen mound. Later NACA studies on the dynamic response of seat structures to impact loads (ref. 3) resulted in a Civil Aeronautics Administration (CAA) update in static seat-strength requirements. The airplanes previously tested by NACA, however, were not structurally representative of current general-aviation airplanes.

In 1973, a general-aviation crash-test program was initiated jointly by the National Aeronautics and Space Administration (NASA) and the Federal Aviation Administration (FAA). (See ref. 4.) As part of this program, the NASA Langley Research Center has conducted a series of crash tests to obtain information on crashes of general-aviation airplanes under controlled free-flight conditions. (See refs. 5 to 10.) These studies are directed toward those crashes in which the airplane structure retains sufficient cabin volume and integrity for occupant survivability. The objectives are to determine the dynamic response of the airplane structures, seats, and occupants during a simulated crash; to determine the effect of flight parameters at impact (i.e., flight speed, flight-path angle, pitch angle, roll angle, and ground condition) on the magnitude and pattern of structural damage; and to determine the loads imposed upon the occupants. This information is essential for

predicting structural collapse and for designing safer seats, safer occupant-restraint systems, and safer cabin structures.

The present tests were conducted to obtain a data base of crash information for four-place, low-wing single-engine airplanes. This report describes the results of three airplane crash tests. Each airplane had a nominal mass of 1043 kg and was impacted at a nominal flight-path velocity of 25 m/sec. Two airplanes were crashed on a concrete surface (at 10° and -30° pitch angles), and one was crashed on soil (at a -30° pitch angle). The pilot, copilot, and passenger were represented by anthropomorphic dummies. Effects of the flight parameters at impact are discussed in terms of structural damage, accelerations of the airplane structure and occupants, and tension in the passenger-restraint system. These data can be used to assess future analytical predictions of stresses, strains, and motions of structural components and seat/occupant behavior.

TEST FACILITY AND PROCEDURES

Facility

The crash tests were performed at the Langley Impact Dynamics Research Facility shown in figure 1. The gantry is composed of truss elements arranged with three sets of inclined legs to give vertical and lateral support and another set of inclined legs to provide longitudinal support. The gantry is 73 m high and 122 m long. The supporting legs are spread 81 m apart at the ground and 20 m apart at the 66-m level. An enclosed elevator and a stairway provide access to the overhead work platforms, and catwalks permit safe traverse of the upper levels of the gantry. A movable bridge spans the gantry at the 66-m level and traverses the length of the gantry. Shown in figure 2 is a sketch of a full-scale airplane specimen suspended from the gantry in the position ready to be swung onto the impact surface. The reinforced-concrete impact surface provides a consistent test surface for repeatability between tests. A soil test-bed approximately 12.1 m wide, 24.4 m long, and 1.2 m deep was placed on the concrete impact surface for one test. The test-bed simulated a plowed field; that is, it was sufficiently firm to support a light tractor with pneumatic tires and soft enough for the airplane to dig into the soil during the crash. (See ref. 11.) Detailed information about the facility is reported in reference 12.

Crash-Test Method

The test method used to crash the airplane specimens is shown schematically in figure 3. The airplane specimen, suspended by two swing cables attached to the top of the gantry, is drawn back and above the impact surface by a pull-back cable to a height of about 49 m. The test sequence begins when the airplane specimen is released from the pull-back cable. The airplane specimen swings pendulum style onto the impact surface. The swing cables are pyrotechnically separated from the airplane specimen when the airplane is about 1 m above the impact surface to free it from restraint during the crash impact. An umbilical cable remains attached during the impact for data acquisition and is pyrotechnically separated about 1/2 sec after ground contact. The umbilical cable links the onboard instrumentation to a data-acquisition system located in a building adjacent to the gantry.

Airplane Suspension System

The airplane suspension system used to control the swing and impact attitude of the airplane specimen is shown in figure 4. The swing and pull-back cables connect to the swing and pull-back harnesses. The swing harness consists of two swing-cable extensions which attach to the wing hard points to support the airplane specimen and to control the roll angle. The pull-back harness consists of a pair of cables attached to the wing hard points and a bar which spreads the cables to clear the airplane fuselage and empennage. The pull-back cable attached to this harness is used to pull the airplane to the height necessary to produce the desired velocity at impact. There are two sets of pitch cables that connect to the swing-cable rings and to fuselage hard points forward and rearward of the airplane center of gravity to control the angle of attack.

Test Parameters

The impact attitude is defined by the test parameters which include the flight-path angle γ, angle of attack α, pitch angle θ, roll angle ϕ, and yaw angle ψ as shown in figure 5. The planned and actual test parameters for the three tests reported here, along with photographs illustrating the impact attitude for each airplane test specimen, are presented in figure 6. Roll and yaw angles had a planned value of zero; thus, for brevity, the test of each airplane is hereinafter identified by word descriptions referring to the pitch angle (i.e., 10° test on concrete, -30° test on concrete, and -30° test on soil) for impact positions shown in figures 6(a) to (c), respectively. The nominal flight-path velocity at impact was 25 m/sec for all tests, which is approximately the stall speed for an airplane of this type.

Airplane Test Specimen

The three airplane specimens used for the tests were identical low-wing, single-engine general-aviation airplanes having a nominal mass of 1043 kg with a capacity for four occupants. (See fig. 7.) The airplane specimens were complete except for the upholstery, empennage, and avionics. The mass and center of gravity of the empennage were simulated by two concentrated masses representing the fin-rudder and stabilizer-elevator combinations. The fuel tanks were filled with water to simulate the fuel mass. Spoilers were attached to the wings to minimize the aerodynamic lift. The exterior and interior of the airplane specimens were painted to enhance the photographic contrast, and black lines were painted over rivet lines to delineate the underlying structure.

The airplanes carried the same basic equipment necessary for the tests. Anthropomorphic dummies, each with a mass of 75 kg, occupied the pilot's, copilot's, and first-passenger's seats. The -30° test on concrete did not include a passenger. The seats were standard for an airplane of this type and were constructed with rigid tubular legs, except in the 10° and -30° tests on concrete in which the copilot's seat was constructed with S-shaped tubular legs. The restraint systems were standard for the pilot and copilot; they consisted of lap belts fastened to the airplane floor and single shoulder harnesses attached between the top of the fuselage and the lap belt. A similar restraint arrangement was used for the passenger in the -30° test on soil. In the 10° test on concrete, no shoulder harness was used on the first passenger, only a lap belt.

INSTRUMENTATION AND DATA PREPARATION

The locations of the accelerometers onboard the airplanes are shown in figure 8. The accelerometers were oriented along the normal (Z), longitudinal (X), and transverse (Y) axes shown in figure 5. Each location is designated by its grid coordinates as follows: the first number indicates the longitudinal coordinates; the first letter indicates the normal coordinate (floor to roof); the second number indicates the transverse coordinate; and the second letter indicates the accelerometer orientation with respect to the airplane body-axis system. The normal and longitudinal orientations are designated as N and L, respectively. For example, the normal-direction accelerometer location on the floor nearest the copilot on the right side of the fuselage is designated 9D10N. The accelerometer locations and their orientation in the dummies are given in the table in figure 8. The orientations of the accelerometers are given in the body-axis system of the dummies, and the locations are given in the grid coordinate system of the airplane.

Data signals were transmitted from the specimen through an umbilical cable to a junction box on top of the gantry, then through hardwire to the control room where they were recorded on frequency-modulation (FM) tape recorders. (See fig. 2.) A time code was recorded simultaneously on the magnetic tape and on the film to synchronize the data signals on the FM tape recorders with the external motion-picture-camera data. There was also a time-pulse generator onboard the airplane for the onboard cameras.

The raw data from the FM tape recorders were digitized and filtered with a 20-Hz and 180-Hz digital filter to remove the higher-frequency local structural vibrations. Calibration information was used to convert the results to engineering units from which acceleration histories were plotted.

RESULTS AND DISCUSSION

10° Test on Concrete

Crash sequence.- The photographs in figure 9 illustrate the crash sequence of a simulated 10° test on concrete (hard landing) from prior to touchdown through initial slide-out. The airplane specimen contacted the concrete impact surface on its main landing gear at a flight-path velocity of 24.6 m/sec along a flight-path angle of -15°, resulting in a sink velocity of 6.4 m/sec. The nose gear then contacted the ground. The airplane settled on the landing gears which caused them to stroke completely and to fracture the left gear (frame 5) and then it continued to slide out at approximately the same attitude as at impact. Inside the cabin, a slight movement of the dummies was seen.

Assessment of damage.- Postcrash photographs of the external damage sustained by the airplane test specimen are presented in figure 10. The livable cabin volume (a volume sufficient in size to maintain space between the occupants and the structure) was maintained during the crash impact. In figure 10(a), the airplane is shown resting on its left wing, right landing gear, and nose wheel. All three tires experienced a blowout. The nose-gear fork bent and twisted as shown in figures 10(a) and (c). The twisted left wing, with no dihedral, the broken linkage for the inboard flap, the sheared rear-spar attachment bolt, and the sheared fore-wing attachment to the fuselage are shown in figures 10(a), (b), (c), and (d), respectively. The fuselage is shown to be in good overall condition except for a slight deformation at the interface with the inboard left-wing flap. Figure 10(e) shows the damaged left land-

ing gear with the fractured shock absorber. Figure 10(f) shows the crew compartment, the pilot and copilot dummies, and their restraints. The overall lack of structural damage by this test is also shown in figure 10(f).

-30° Test on Concrete

Crash sequence.- The photographs in figure 11 illustrate the crash sequence of a -30° pitch (nose-down) impact test starting prior to touchdown through a part of the slide-out. The airplane specimen contacted the concrete impact surface on its nose wheel at a flight-path velocity of 24.6 m/sec (sink velocity of 11.9 m/sec (frame 4)). The nose gear then collapsed (frame 5) and finally embedded in the floor in the baggage compartment (cabin cargo area). Afterwards, the airplane nose, followed by the main landing gears, contacted the ground. As the airplane continued its travel, the fuselage rotated downward, the airplane nose crushed, and the main landing gears collapsed which forced the wings to twist (frame 6). At the onset of the decelerating forces (frame 5), the pilot and copilot started to pitch forward and their upper torso lurched toward the instrument panel (frames 6 and 7). Most of the crushing and damage to the airplane took place at the time recorded in frame 6. Frames 7, 8, and 9 show the airplane settling on the impact surface and sliding out.

Assessment of damage.- Postcrash photographs of the damage sustained by the airplane specimen are shown in figure 12. Figure 12(a) shows the airplane in its final position resting on the fuselage and wings. The nose and main landing gears fractured and collapsed and the tires blew out during the impact. Both windshields broke and the center post between the windshields bent. Some of the front damage can be seen under the engine cowling. The impact force caused part of the lower fire wall to protrude about 20 cm into the cabin. Both wings lost their dihedral, and the left wing is shown propped by the collapsed landing gear. The balloon seen in figure 12(a) was part of an Emergency Locator Transducer (ELT) experiment for locating a crashed airplane by visible means.

Figure 12(b) shows the pilot and copilot dummies restrained to their seats after the airplane came to a stop. Also shown is buckling of the airplane nose and side panel over the wing. The space between the seats and instrument panel, as well as the livable cabin volume, was maintained. Figure 12(c) shows the left inboard-flap control broken, the rear-spar attachment pin sheared off, and some buckling in the fuselage skin. Figure 12(d) shows a collapsed landing gear and buckling of the skin under and aft of the cargo door. In figure 12(e), the nose wheel is seen embedded in the floor of the rear cabin. Also shown is the rear-cabin-floor upheaval aft of the passenger compartment, the transducer junction box, and the pyrotechnic programmer box. Figure 12(f) shows a slight deformation in the aft member of the doorframe and a fracture in the lower front corner. Other damage to the airplane, not shown in these photographs, was buckled skin from the airplane nose to the third left window, a buckled wing at the attachment point to the fuselage forward of the main spar, a cracked first-passenger window, a collapsed left landing gear, and a failed copilot seat rail at the rear-legs attachment point.

-30° Test on Soil

Crash sequence.- The crash sequence of a -30° pitch (nose-down) impact test on a soil surface is illustrated in figure 13. The sequence starts prior to touchdown and ends when the scattered soil starts to settle after the abrupt impact. The airplane specimen contacted the soil impact surface on its nose wheel at a flight-path veloc-

ity of 24.6 m/sec (a sink velocity of 12.9 m/sec). The nose gear then collapsed (frame 2) and later lodged in the lower half of the fire wall during crushing of the airplane nose. The nose of the airplane started to crush (frame 3), and the main landing gears contacted the ground.

As the airplane decelerated, the dummies started to pitch forward (frame 3) and lurched forward out of the view in frame 4. The pilot's shoulder harness can be seen taut and fully extended holding the displaced dummy (frame 4). Frame 4 also shows that the nose of the airplane has crushed to the fire wall, the engine cowling has come off, the landing gears have collapsed, the wings have contacted the ground, and buckling of the structure has occurred on the top and side of the fuselage.

Frame 5 shows further compression of the fuselage with heavy damage extending up to the pilot's window. The aft part of the left wing has started to separate from the fuselage. Bending of the roof has occurred aft of the pilot's window, and the engine cowling has completely separated from the airplane. The pilot and copilot dummies have bounced back to the seated position, and fire wall has protruded into the crew area, thus reducing the space between the fire wall and the crew seats. The first-passenger dummy is bent forward over its knees and, in frame 6, has started to rebound. The left wing continues to separate from the fuselage at the main spar while pivoting forward. In frame 7, the wing has separated from the main spar and more recovery in the first-passenger dummy is shown. Frame 8 shows the pilot dummy flexing forward, the first-passenger dummy slanted forward at 45° and moving rearward, and the left wing completely detached from the fuselage. In frame 9, the pilot dummy is flexing rearward and the first-passenger dummy is bouncing upward and rearward.

In frames 10 and 11, the first-passenger-dummy's head has hit the roof while moving rearward in an arc. In frames 12 and 13, the first-passenger-dummy's head is no longer in contact with the roof and the upper torso continues to rotate rearward. The pilot dummy is seen flexing forward. In frames 14, 15, and 16, the pilot and copilot dummies are shown pitched forward into the instrument panel. The first-passenger dummy is shown against the seat back.

Assessment of damage.- Postcrash photographs of the damage sustained by the airplane specimen are shown in figure 14. The livable cabin volume, although reduced, was maintained during the crash impact. Figure 14(a) shows the airplane in its final position resting on the fuselage and right wing. The left wing is shown detached and in front of the airplane. The engine top cowling has come off and is shown on the right side ahead of the wing. Figure 14(b) shows buckles on the wing leading edge and on the side panel ahead of the door, and also shows damage to the nose, windshields, and center post of the airplane. The degree of center-post bend is an indication of the protrusion of the fire wall into the cabin. The protrusion of the lower half of the fire wall into the cabin measured up to 51 cm and was more severe than the top half. Figure 14(c) shows a tear on the wing over the landing gear, separation of the right wing from the fuselage aft of the main spar, a fracture in the lower rear of the doorframe, and the copilot-dummy's knees bent up due to the reduced space from the seat to the fire wall. Figure 14(d) shows a bent propeller, a bent and fractured engine mount, a torn lower engine cowling, and a deformed fire wall. Figure 14(e) shows a fractured main-spar attachment to the wing and the broken hydraulic lines in the left wing. Figure 14(f) shows the floor and foot-control deformations in the copilot's side of the fuselage.

Other damage not shown in figure 14 were heavy buckling in the pilot's side of the fuselage and shearing of rivets in the left part of the roof to the left of the

pilot's window. It was also noticed that the pilot's window broke off, the pilot's seat pan tore through, and part of the pilot's control wheel fractured off.

Normal Accelerations

Cabin floor.- Normal accelerations on the cabin floor in the crew and passenger compartments for the three tests are presented in figure 15. The crew compartment is located forward of the main spar, and the passenger compartment is located immediately aft of the main spar. Floor accelerometers were placed adjacent to each leg of the pilot's seat, to the right rear leg of the copilot's seat, and to the front inboard leg of the first-passenger's seat. To obtain an overall acceleration value for the cabin floor in each test, three peak accelerations on the inboard floor beam located under the seats of the pilot and first passenger were averaged and compared. The beam was chosen for its location (toward the center of the fuselage) and for its rigidity (accelerations less susceptible to local deformations). In the discussion that follows, it should be noted that only the first significant acceleration peaks are being compared.

The normal accelerations in the crew compartment for the 10° test on concrete were evenly distributed from wall to wall and peaked at -11g. In the passenger compartment, a -15g peak acceleration was obtained. The average peak acceleration on the floor beam was -13g.

Normal peak accelerations in the cabin for the -30° test on concrete ranged in values from -25g to -37g. In the crew compartment, peak accelerations varied between -31g and -37g; whereas in the passenger compartment, they varied between -25g and -28g. The average peak acceleration on the floor beam was -29g.

Normal peak accelerations in the crew compartment for the -30° test on soil ranged between -6g and -19g, with the higher peak accelerations obtained toward the aisle. Lower values (-6g to -13g) were obtained toward the cabin wall. In the passenger compartment a peak acceleration of -12g was obtained near the aisle. The average peak acceleration on the floor beam was -17g.

Cabin roof, fuselage tail, and left wing.- Normal peak accelerations on the cabin roof, fuselage tail, and left wing are presented in figure 16. Peak accelerations on the roof in the crew compartment averaged -12g for the 10° test on concrete, -31g for the -30° test on concrete, and -10g for the -30° test on soil. On the tail, the peak accelerations, apparently because of the structural flexibility, varied from 20g to -12g for the 10° test on concrete, 19g to -27g for the -30° test on concrete, and 10g to -11g for the -30° test on soil. On the wing, a -5g peak acceleration occurred at impact for the -30° test on soil, with a maximum acceleration of 39g as the wings were torn from the fuselage. Wing accelerations for the other two tests were not recorded.

Engine compartment, main spar, and luggage compartment. Normal accelerations in the engine compartment, main spar, and luggage compartment are presented in figure 17. Normal accelerometers mounted on the engine recorded -12g in the 10° test on concrete, -52g in the -30° test on concrete, and -18g for the -30° test on soil. On the fire wall, the average peak accelerations were -12g, -20g, and -25g, respectively; on the main spar, they were -12g, -25g, and -9g, respectively; and in the luggage compartment, they were -11g, -13g, and -7g, respectively. In general, the normal peak accelerations at these locations were highest for the -30° test on concrete, with the exception of an accelerometer on the middle of the fire wall that

recorded a higher acceleration for the -30° test on soil. However, this was a localized acceleration value at the deformation site and not an average acceleration. In the engine compartment and at the main spar, accelerations were lowest for the 10° test on concrete. In the luggage compartment, accelerations were lowest for the -30° test on soil.

Pilot's body and seat pan.- Normal accelerations in the pilot's body and seat pan are presented in figure 18. In the 10° test on concrete, peak accelerations of -20g and -22g were recorded in the pilot's head and pelvis, respectively. A peak acceleration of -14g was recorded at the seat pan. No acceleration was recorded on the pilot's chest for this test. In the -30° test on concrete, a peak acceleration of -37g was recorded at the pilot's seat pan. No accelerations were recorded at the head, chest, or pelvis. In the -30° test on soil, peak accelerations of 155g, -168g, -46g, and -8g were recorded in the pilot's head, chest, pelvis, and seat pan, respectively. From a high-speed motion-picture analysis, it was observed that during the impact of the airplane on the soil, the dummy's head impacted the instrument panel on the right side of the control stick. The high positive acceleration value (155g) recorded in the head and the negative value (-168g) in the chest are a consequence of this impact. The normal acceleration of -8g in the seat pan occurred primarily because the soil impact was essentially a high longitudinal loading in which the dummies' moving forward unloaded the seat-pan area.

Copilot's pelvis and seat pan.- Normal accelerations in the copilot's pelvis and seat pan are presented in figure 19. In the 10° test on concrete, the peak acceleration recorded in the dummy's pelvis was -4g and in the seat pan was -14g. In the -30° test on concrete, the peak acceleration recorded in the pelvis was -29g and in the seat pan was -20g. Acceleration data at these locations were lost for the -30° test on soil.

Longitudinal Accelerations

Cabin floor.- Longitudinal accelerations on the cabin floor in the crew and passenger compartments in the vicinity of the pilot, copilot, and first-passenger locations for the three tests are presented in figure 20. Peak accelerations taken at three locations along the inboard floor beam under the pilot and first passenger were averaged for each test to obtain a representative cabin-floor peak acceleration. Average floor peak acceleration were -2g for the 10° test on concrete, -11g for the -30° test on concrete, and -26g for the -30° test on soil. Local accelerations for each test were distributed rather evenly both in the crew compartment and across the floor beam. Longitudinal accelerations are a function of the velocity change during initial impact. The tests with longer slide-out distances produced lower longitudinal accelerations because a lower longitudinal velocity change occurred at initial impact.

Cabin roof, fuselage tail, and left wing.- Longitudinal accelerations on the cabin roof, fuselage tail, and left wing are presented in figure 21. The highest accelerations were recorded for the -30° test on soil, and the lowest were for the 10° test on concrete. On the cabin roof, peak accelerations were small and varied from 5g to -5g for the 10° test on concrete, 8g to -17g for the -30° test on concrete, and 9g to -22g for the -30° test on soil. Accelerations at the Emergency Locator Transducer (ELT) location were -3g, -8g, and -14g for the 10° test on concrete, the -30° test on concrete, and the -30° test on soil, respectively; whereas on the tail at the fuselage top, the peak accelerations were -5g, -15g, and -25g,

respectively. On the left wing, the peak acceleration was -22g for the -30° test on soil. No accelerations were recorded on the wing for the other tests.

Engine compartment, main spar, and luggage compartment.- Longitudinal accelerations in the engine compartment, main spar, and luggage compartment are presented in figure 22. Peak longitudinal accelerations recorded on the engine were -5g for the 10° test on concrete, -24g for the -30° test on concrete, and -77g for the -30° test on soil. For the 10° test on concrete, peak accelerations were -2g on the lower left portion of the fire wall and -3g on the middle portion. For the -30° test on concrete, the peak accelerations were -14g and -38g, respectively. Fire-wall data were lost for the -30° test on soil. In the main spar, the longitudinal peak accelerations were -4g for the -10° test on concrete, -13g for the -30° test on concrete, and -30g for the -30° test on soil. In the luggage compartment, the peak accelerations were -5g, -12g, and -27g, respectively. In general, the acceleration magnitudes at these locations were highest for the test on soil and lowest for the 10° test on concrete.

Pilot dummy.- Longitudinal accelerations in the pilot's head, chest, and pelvis are presented in figure 23. In the pilot's head, a peak acceleration of -5g was obtained in the 10° test on concrete. In the -30° test on concrete, a partial acceleration trace with a value of -40g was obtained before the data were lost. An acceleration of -240g occurred in the -30° test on soil because high-speed motion-pictures for this test showed the pilot's head striking the instrument panel. A high-acceleration spike of short duration is indicative of such an impact. In the pilot's chest, the longitudinal peak accelerations were -12g in the 10° test on concrete, -33g in the -30° test on concrete, and -24g in the -30° test on soil. In the pilot's pelvis, the longitudinal peak accelerations were -6g in the 10° test on concrete, -23g in the -30° test on concrete, and -60g in the -30° test on soil. No longitudinal accelerations were measured in the copilot dummy.

Tension in Restraint-Harness System

Tension for the lap belt and shoulder harness in the pilot and copilot dummies are shown in figure 24. Loads in the pilot's lap belt were negligible for the 10° test on concrete, 200 N for the -30° test on concrete, and 3700 N for the -30° test on soil. In the pilot's shoulder harness, the loads were negligible for the 10° test on concrete, 3400 N for the -30° test on concrete, and 3800 N for the -30° test on soil. In the copilot's lap belt and shoulder harness, the loads were negligible for the 10° test on concrete; but they were 1400 N and 3000 N, respectively, for the -30° test on concrete. For the -30° test on soil, no measurements were made on the copilot's lap belt and shoulder harness. Attempts to correlate restraint loads with accelerations of the dummies and seats were not made because loads are measured in directions other than the accelerations, seat/occupant interactions may be different for different seats under the same apparent loadings, and dummies striking the airplane structure alter drastically the various responses of dummies and seats.

CONCLUDING REMARKS

Three identical four-place, low-wing single-engine airplane specimens were crash-tested at the Langley Impact Dynamics Research Facility. Two airplanes were crashed on a concrete surface at 10° and -30° pitch angles, and one airplane was crashed on soil at a -30° pitch angle. The purpose of the tests was to determine the

structural and occupant response for low-wing single-engine airplane specimens at three different impact conditions. All airplane specimens were tested at the same nominal impact velocity of 25 m/sec along the flight path.

In all three tests, the livable volume inside the cabin was sufficiently maintained to provide protection for the occupants. The worst cabin interior damage occurred in the test on soil where the fire wall protruded up to 51 cm into the cabin. Exterior damage to the airplane was also most severe in the test on soil where the engine compartment and fire wall sustained massive structural damage, the left wing detached, and the nose and landing gears collapsed. Severe damage, but of lesser magnitude, occurred in the -30° test on concrete where the fire wall protruded slightly into the cabin, the nose wheel embedded in the luggage-compartment floor, and the nose and main landing gears collapsed. The least structural damage occurred for the 10° test on concrete because most of the impact energy was dissipated by the landing gears and by friction during the long slide-out distance. A common damage in all three tests was a bolt failure in the rear wing-spar bracket.

On the cabin floor, average accelerations in the normal direction were -13g for the 10° test on concrete, -29g for the -30° test on concrete, and -17g for the -30° test on soil. In the longitudinal direction, the average cabin-floor accelerations were -2g for the 10° test on concrete, -11g for the -30° test on concrete, and -26g for the -30° test on soil. Normal peak accelerations in the pilot's head were -20g for the 10° test on concrete and 155g for the -30° test on soil (due to the dummy's striking the airplane structure).

Normal peak accelerations in the pilot's seat pan were -14g for the 10° test on concrete, -37g for the 30° test on concrete, and -8g for the 30° test on soil. The pilot's lap-belt tension was 200 N for the -30° test on concrete and 3700 N for the -30° test on soil. For the 10° test on concrete, the lap-belt tension was negligible. Longitudinal accelerations in the pilot's pelvis were -6g for the 10° test on concrete, -23g for the -30° test on concrete, and -60g for the -30° test on soil.

Langley Research Center
National Aeronautics and Space Administration
Hampton, VA 23665
August 2, 1983

REFERENCES

1. Preston, G. Merritt; and Moser, Jacob C.: Crash Loads. NACA Conference on Airplane Crash-Impact Loads, Crash Injuries and Principles of Seat Design for Crash Worthiness, Apr. 1956, pp. 2-1 - 2-47. (Available as NASA TM X-60777.)

2. Eiband, A. Martin; Simpkinson, Scott H.; and Black, Dugald O.: Accelerations and Passenger Harness Loads Measured In Full-Scale Light-Airplane Crashes. NACA TN 2991, 1953.

3. Pinkel, I. Irving; and Rosenberg, Edmund G.: Seat Design for Crash Worthiness. NACA Rep. 1332, 1957. (Supersedes NACA TN 3777.)

4. Hayduk, Robert J.; Thomson, Robert G.; and Carden, Huey D.: NASA/FAA General Aviation Crash Dynamics Program - An Update. Forum, vol. 12, no. 3, Winter 1979, pp. 147-156.

5. Alfaro-Bou, Emilio; and Vaughan, Victor L., Jr.: Light Airplane Crash Tests at Impact Velocities of 13 and 27 m/sec. NASA TP-1042, 1977.

6. Castle, Claude B.; and Alfaro-Bou, Emilio: Light Airplane Crash Tests at Three Flight-Path Angles. NASA TP-1210, 1978.

7. Castle, Claude B.; and Alfaro-Bou, Emilio: Light Airplane Crash Tests at Three Roll Angles. NASA TP-1477, 1979.

8. Vaughan, Victor L., Jr.; and Alfaro-Bou, Emilio: Light Airplane Crash Tests at Three Pitch Angles. NASA TP-1481, 1979.

9. Vaughan, Victor L., Jr.; and Hayduk, Robert J.: Crash Tests of Four Identical High-Wing Single-Engine Airplanes. NASA TP-1699, 1980.

10. Williams, M. Susan; and Fasanella, Edwin L.: Crash Tests of Four Low-Wing Twin-Engine Airplanes With Truss-Reinforced Fuselage Structure. NASA TP-2070, 1982.

11. Cheng, Robert Y. K.: Soil Analyses and Evaluations at the Impact Dynamics Research Facility for Two Full-Scale Aircraft Crash Tests. NASA CR-159199, 1977.

12. Vaughan, Victor L., Jr.; and Alfaro-Bou, Emilio: Impact Dynamics Research Facility for Full-Scale Aircraft Crash Testing. NASA TN D-8179, 1976.

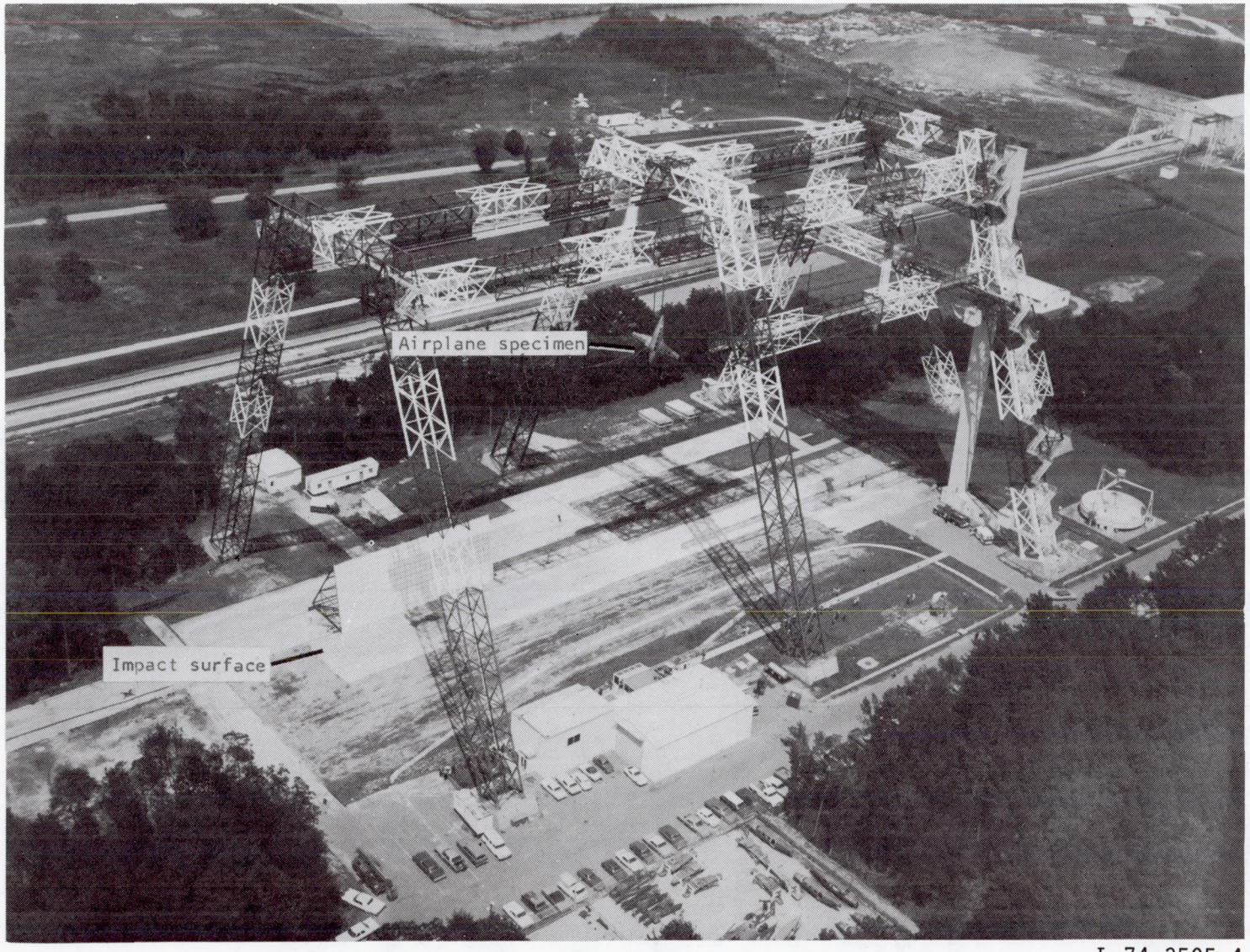

L-74-2505.4

Figure 1.- Langley Impact Dynamics Research Facility.

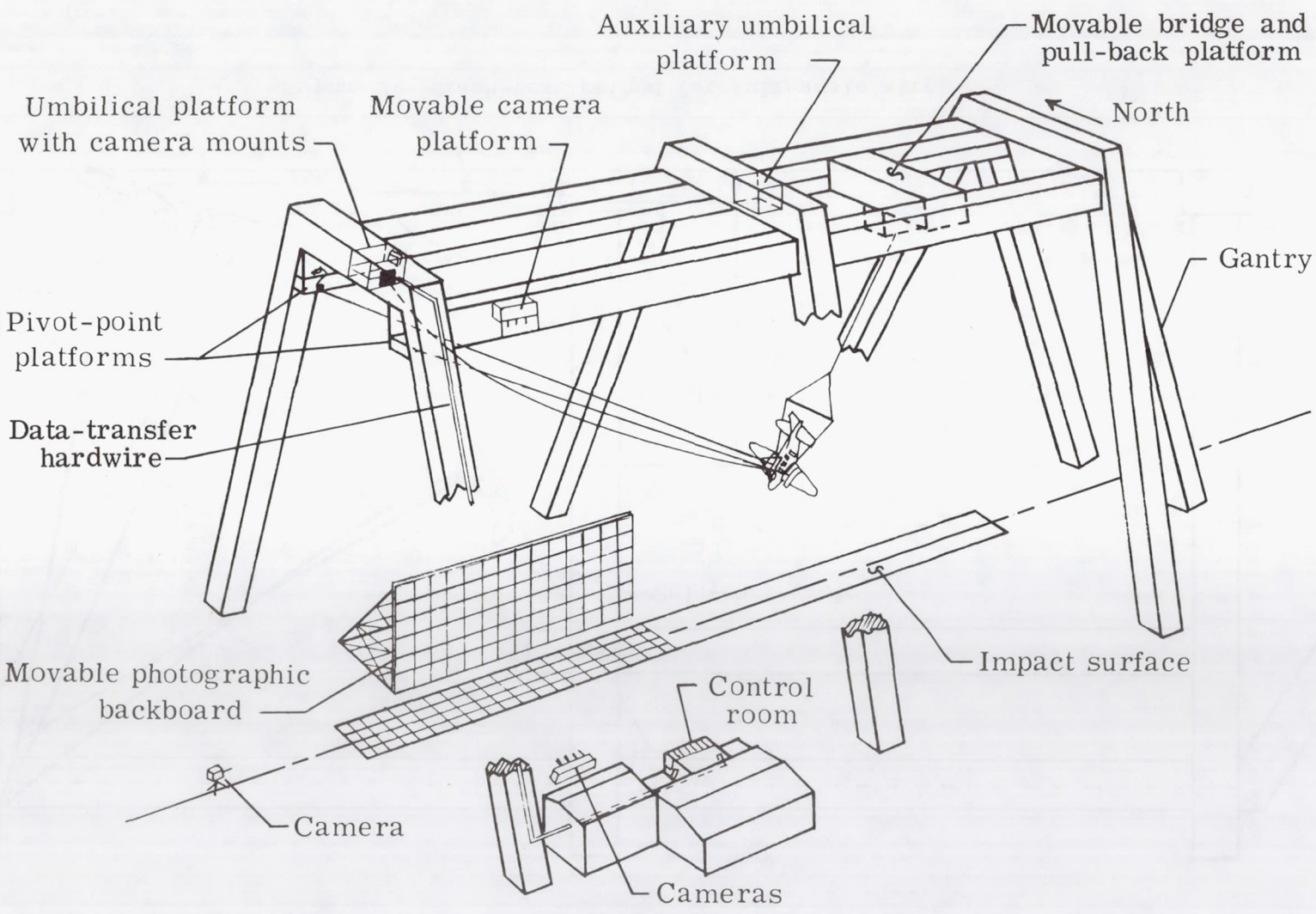

Figure 2.- Diagram of Langley Impact Dynamics Research Facility.

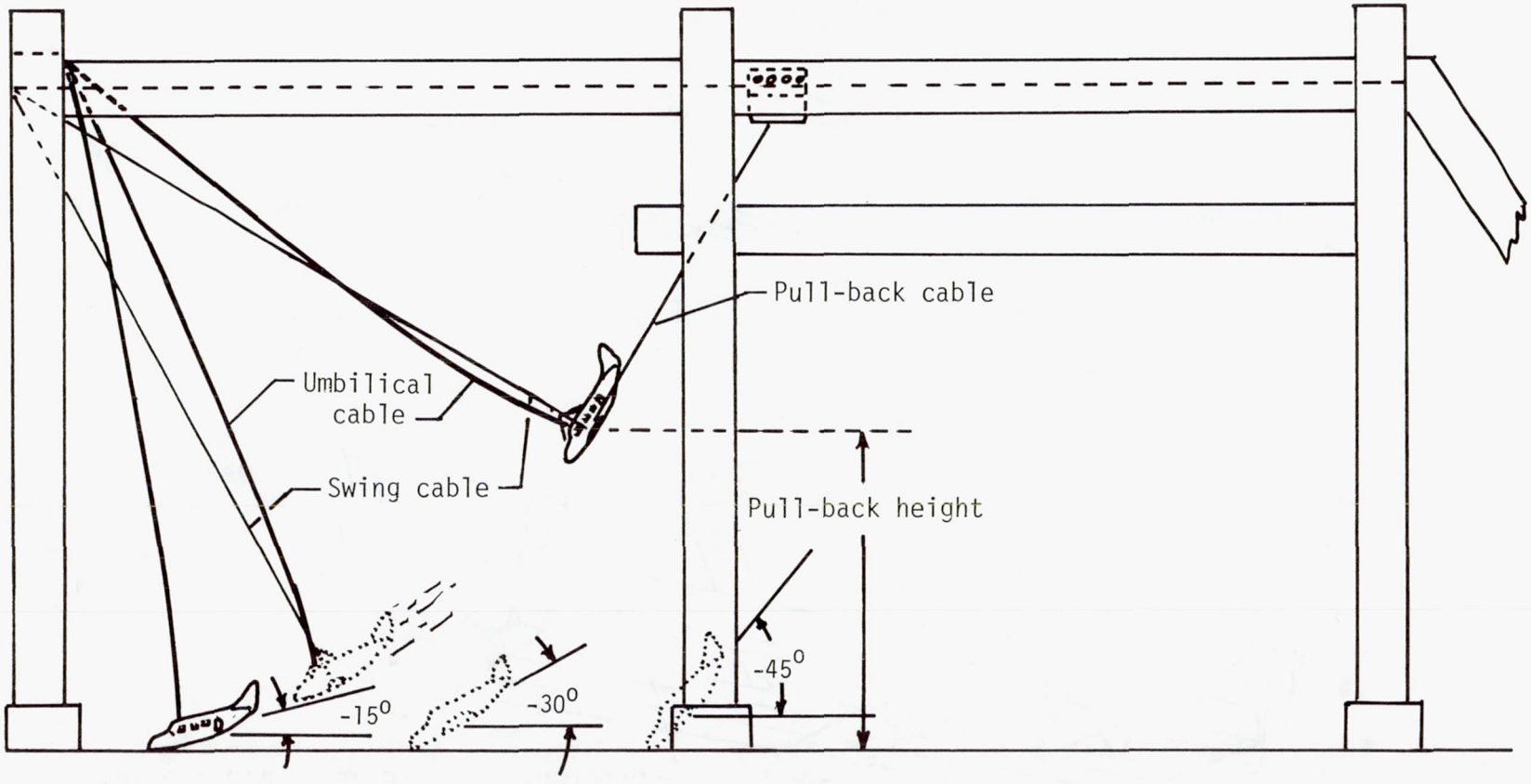

Figure 3.- Crash-test method for full-scale airplane.

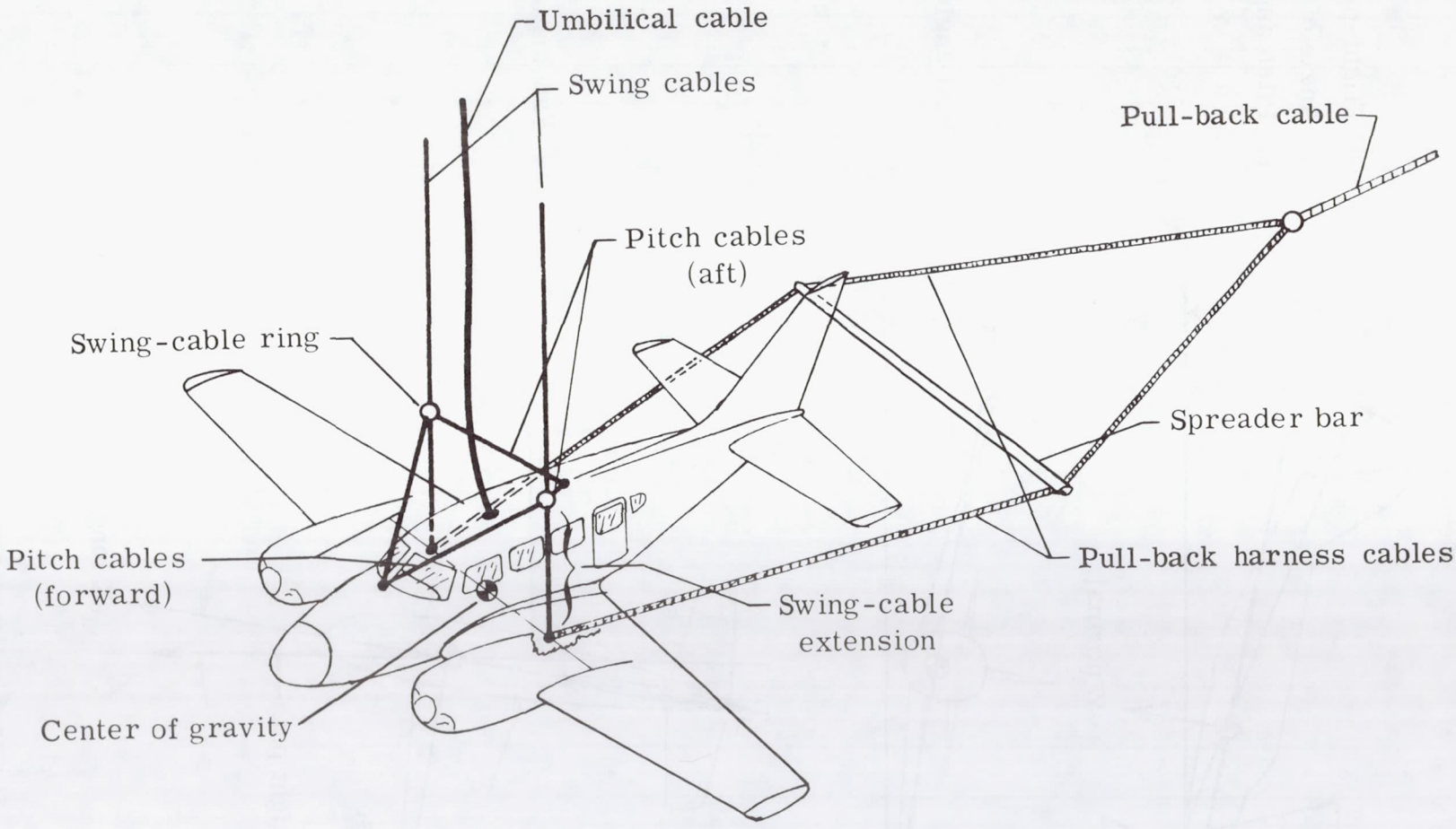

Figure 4.- Airplane suspension system.

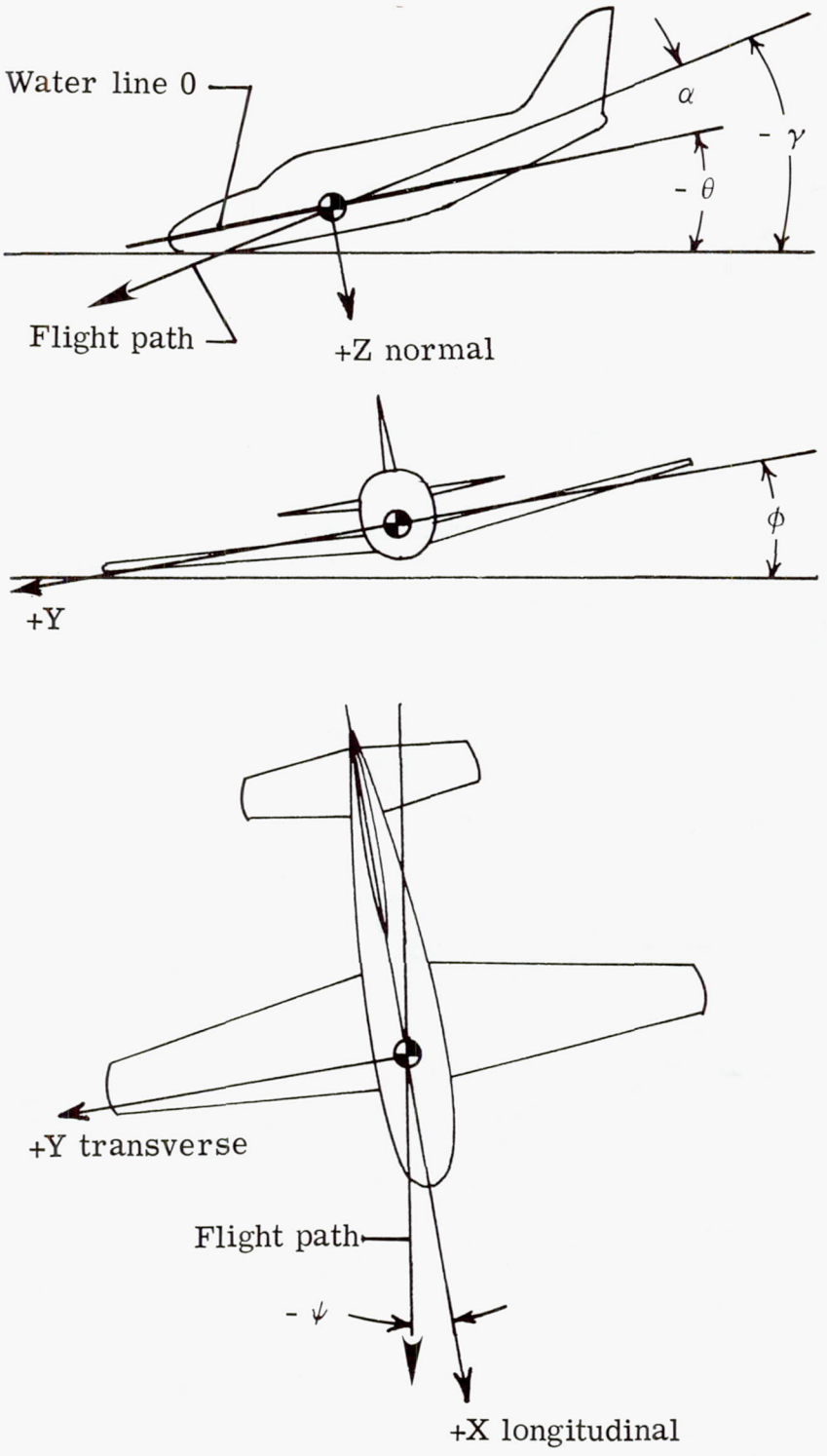

γ Flight-path angle

α Angle of attack

θ Pitch angle,

$\theta = \gamma + \alpha$

ϕ Roll angle

ψ Yaw angle

Figure 5.- Coordinate system and crash attitude.

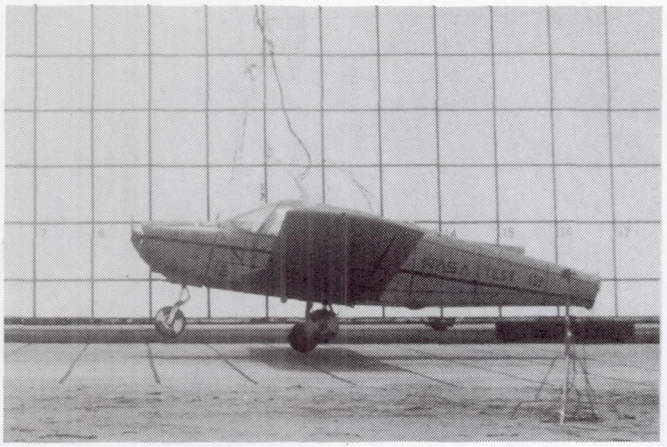

Test parameter	Planned	Actual
Flight-path angle, γ, deg	-15	-15
Angle of attack, α, deg	25	24
Pitch angle, θ, deg	10	9
Roll angle, ϕ, deg	0	4.3
Yaw angle, ψ, deg	0	1.8
Flight-path velocity, m/sec	24.6	25

(a) 10° test on concrete.

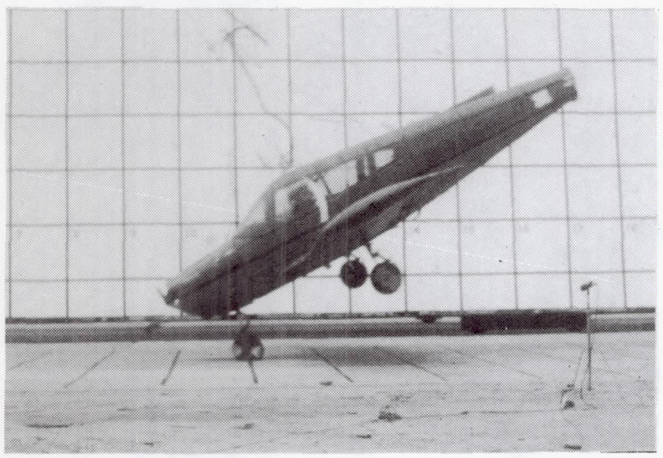

Test parameter	Planned	Actual
Flight-path angle, γ, deg	-30	-29
Angle of attack, α, deg	0	3
Pitch angle, θ, deg	-30	-26
Roll angle, ϕ, deg	0	-1
Yaw angle, ψ, deg	0	-3
Flight-path velocity, m/sec	24.6	24.6

(b) -30° test on concrete.

L-83-101

Test parameter	Planned	Actual
Flight-path angle, γ, deg	-30	-31
Angle of attack, α, deg	0	3.8
Pitch angle, θ, deg	-30	-27.3
Roll angle, ϕ, deg	0	2.5
Yaw angle, ψ, deg	0	-7.3
Flight-path velocity, m/sec	24.6	25

(c) -30° test on soil.

Figure 6.- Test specimens and test parameters.

L-77-7029

Figure 7.- Typical airplane test specimen in crash-test preparation.

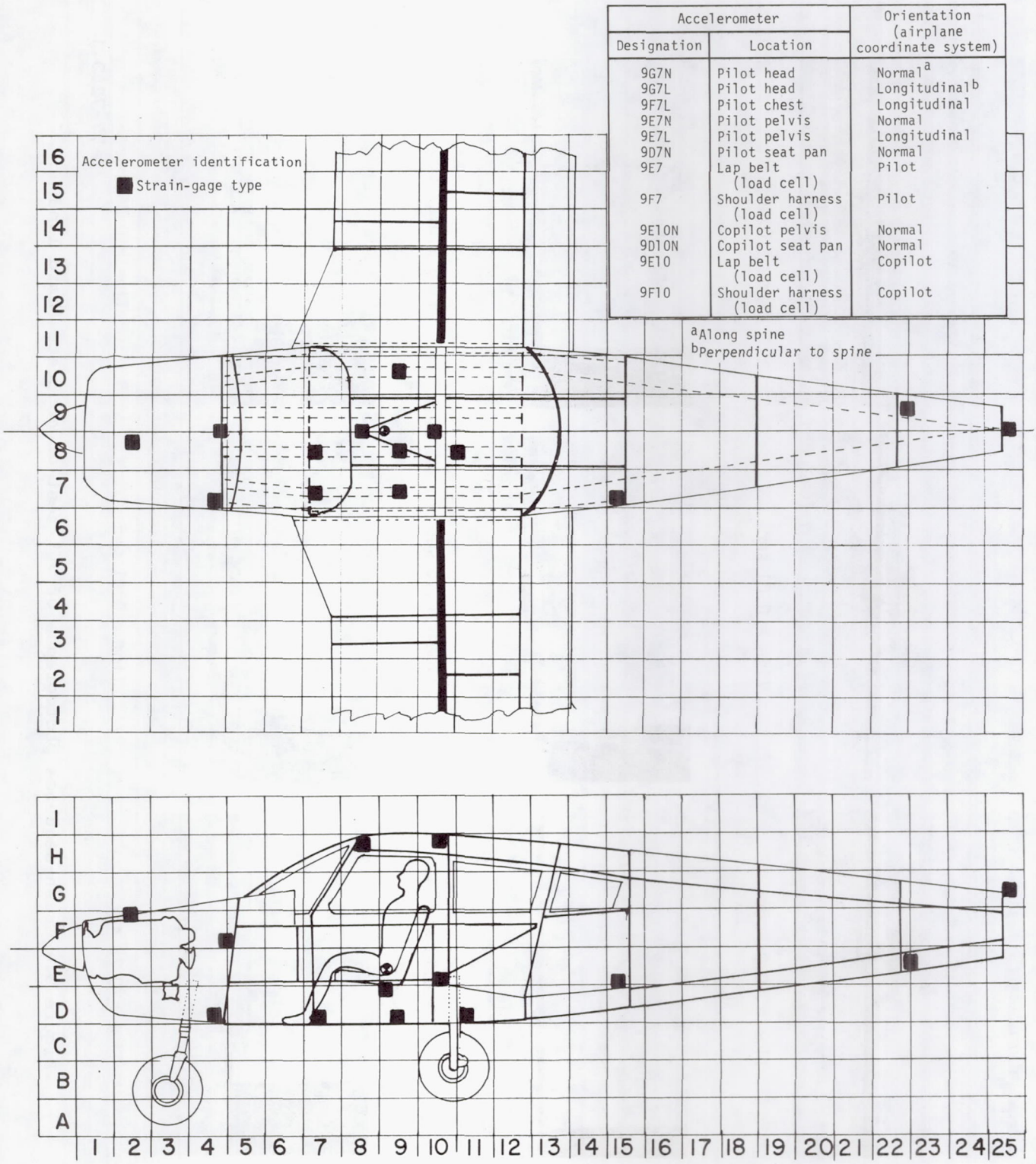

Accelerometer		Orientation (airplane coordinate system)
Designation	Location	
9G7N	Pilot head	Normal[a]
9G7L	Pilot head	Longitudinal[b]
9F7L	Pilot chest	Longitudinal
9E7N	Pilot pelvis	Normal
9E7L	Pilot pelvis	Longitudinal
9D7N	Pilot seat pan	Normal
9E7	Lap belt (load cell)	Pilot
9F7	Shoulder harness (load cell)	Pilot
9E10N	Copilot pelvis	Normal
9D10N	Copilot seat pan	Normal
9E10	Lap belt (load cell)	Copilot
9F10	Shoulder harness (load cell)	Copilot

Figure 8.- Diagram of accelerometer locations on airplane structure and in dummies.

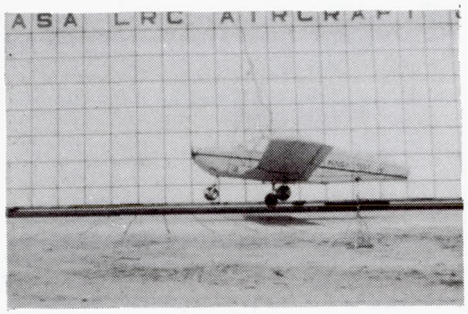

Time = -0.04 sec

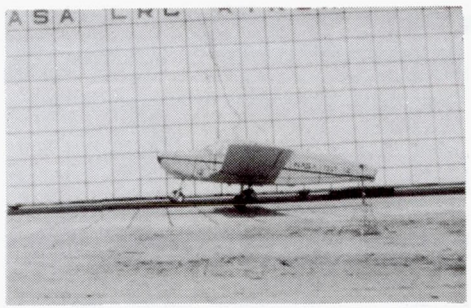

Time = 0.01 sec

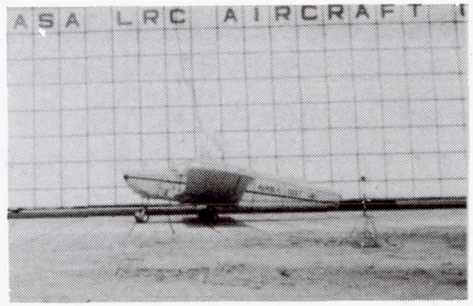

Time = 0.06 sec

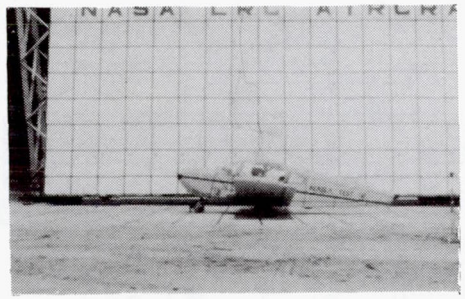

Time = 0.11 sec

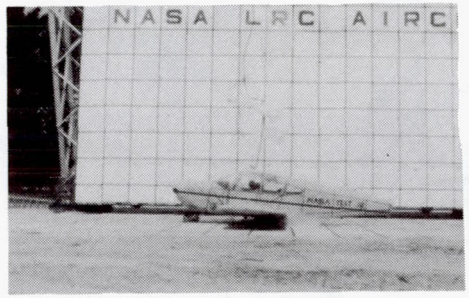

Time = 0.16 sec

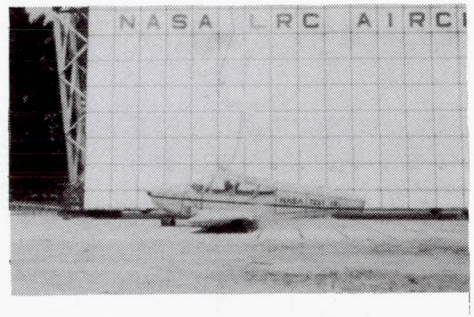

Time = 0.21 sec

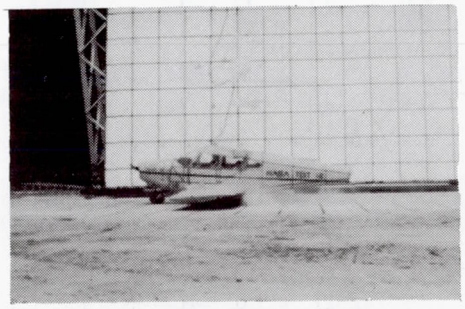

Time = 0.26 sec

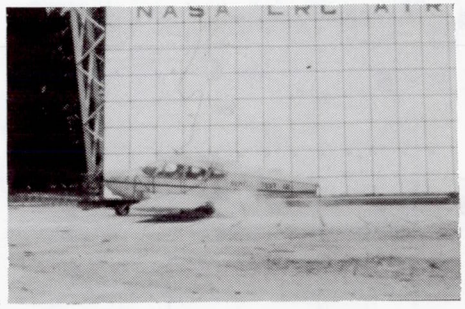

Time = 0.31 sec

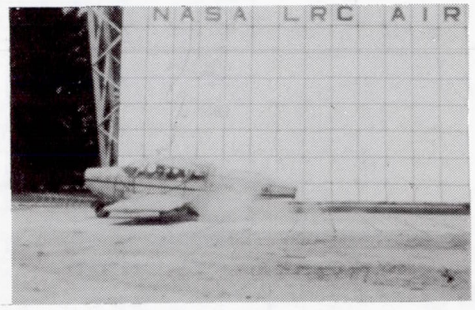

Time = 0.36 sec

L-77-7203.1

Figure 9.- Crash-sequence photographs of 10° test on concrete (hard landing).

(a) Overall view from front.

(b) Overall view from rear.

(c) Overall view from left side.

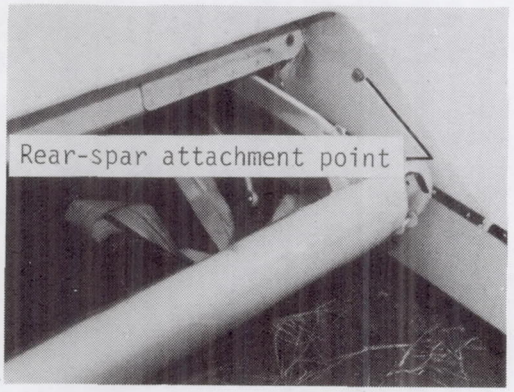

(d) Close-up view of rear-spar attachment.

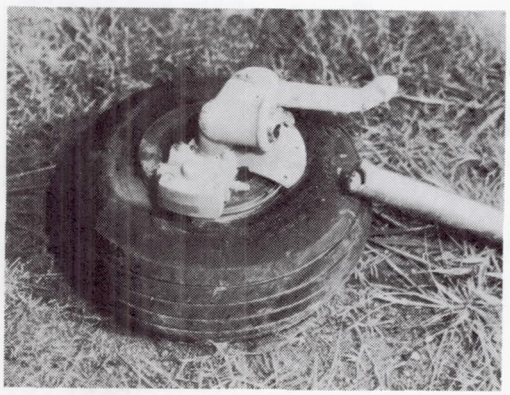

(e) Close-up view of left main gear.

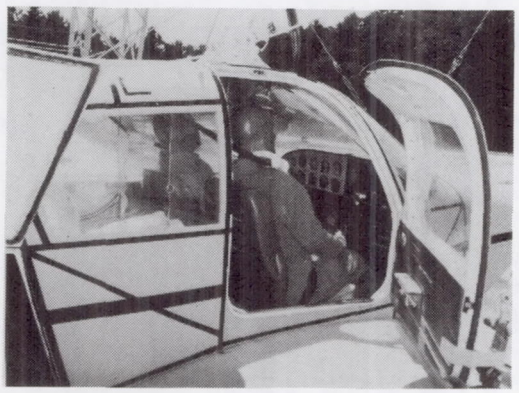

(f) Close-up view of crew compartment from right side.

L-83-102

Figure 10.- Postcrash external damage to test specimen in 10° test on concrete (hard landing).

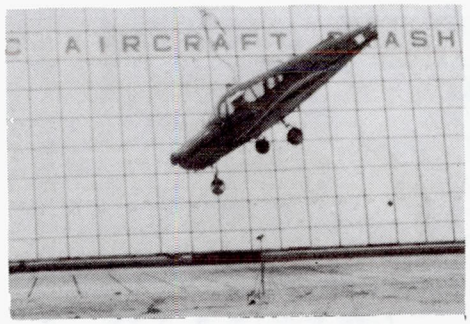

Time = -0.14 sec

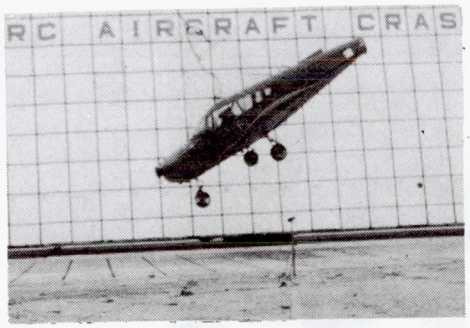

Time = -0.09 sec

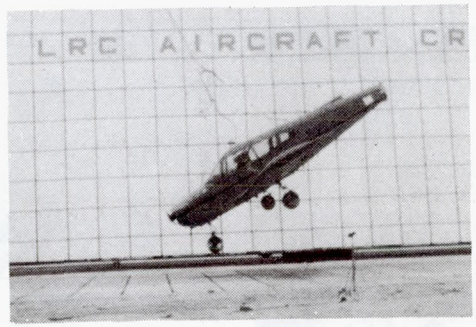

Time = -0.04 sec

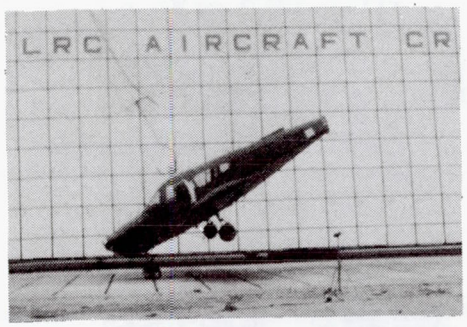

Time = 0.01 sec

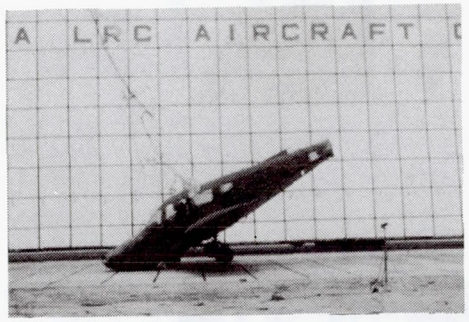

Time = 0.06 sec

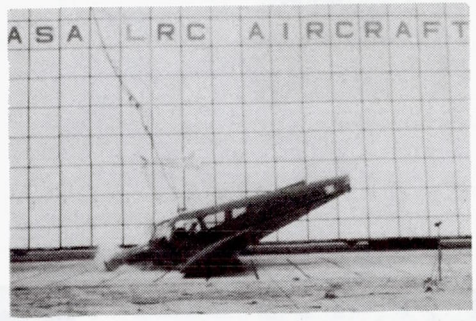

Time = 0.11 sec

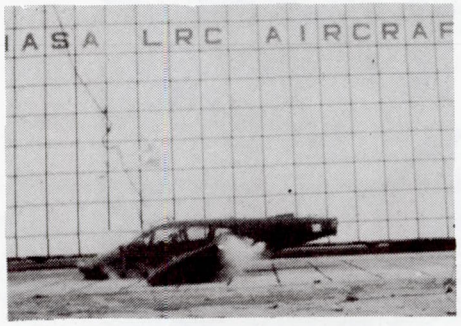

Time = 0.16 sec

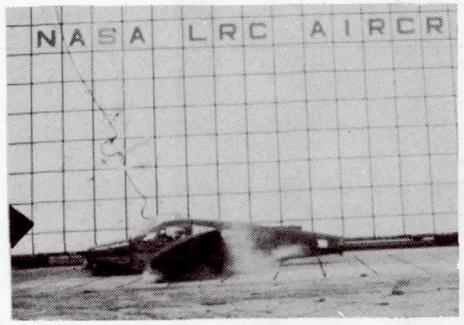

Time = 0.21 sec

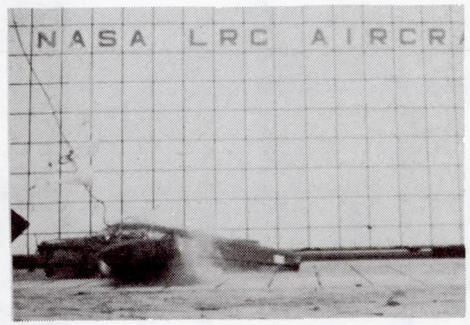

Time = 0.26 sec

L-78-315.1

Figure 11.- Crash-sequence photographs of -30° (nose-down) test on concrete.

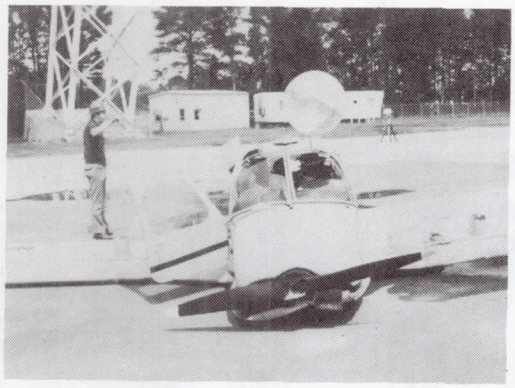

(a) Overall view from front.

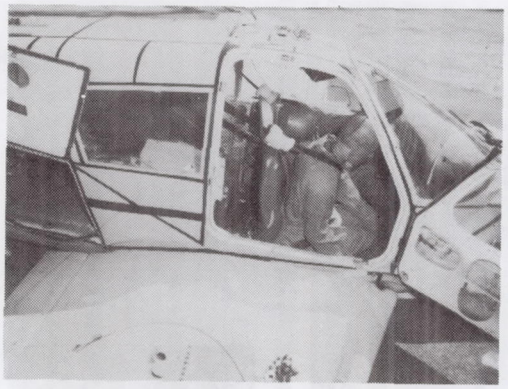

(b) Close-up view of forward section from right side.

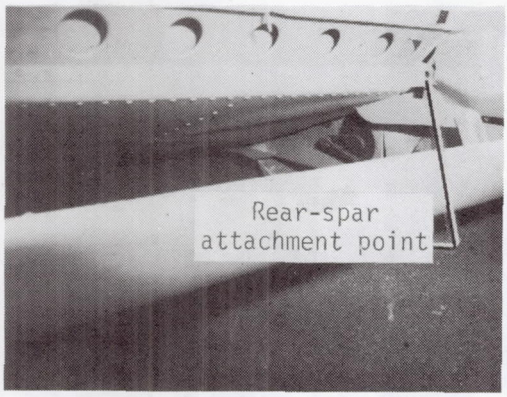

(c) Close-up view of rear-spar attachment.

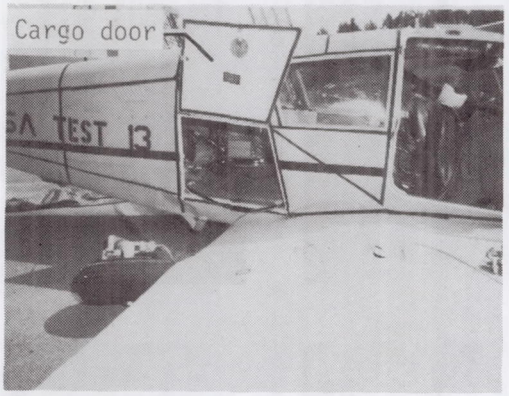

(d) Close-up view of right wing and cabin section.

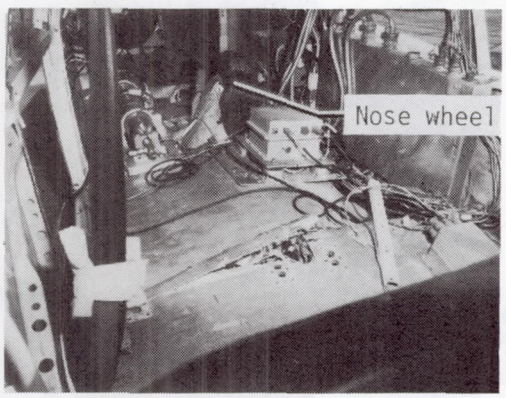

(e) Close-up view of rear-cabin area.

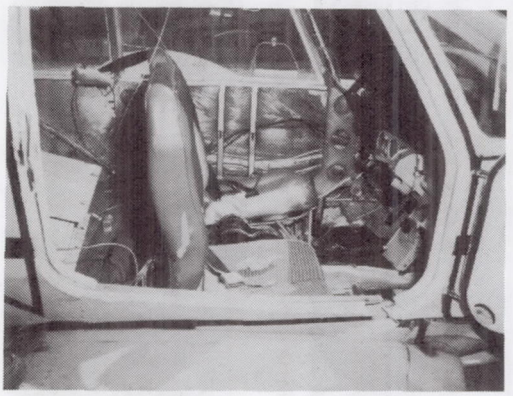

(f) Close-up view of crew section.

L-83-103

Figure 12.- Postcrash damage to test specimen in -30° (nose-down) test on concrete.

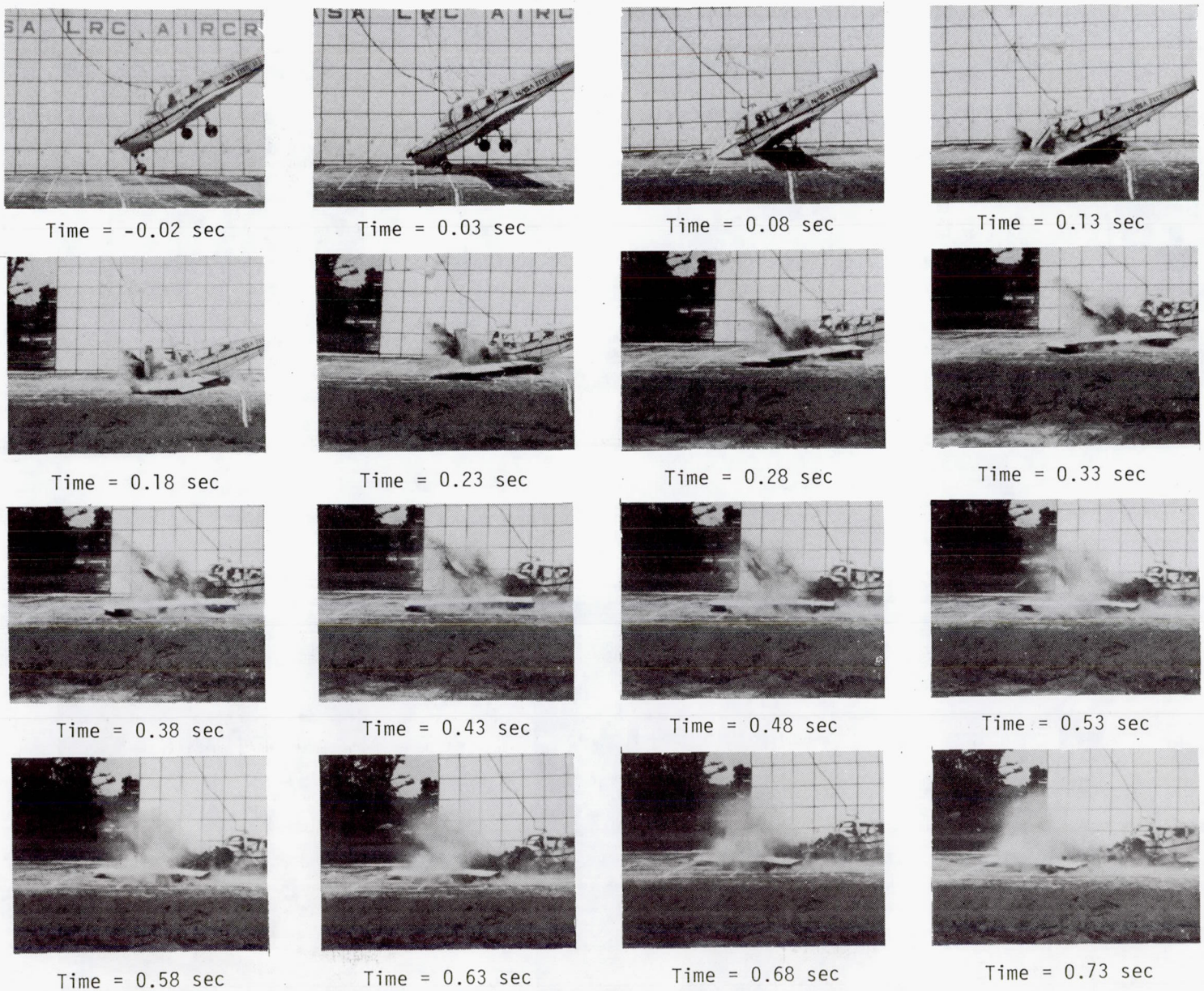

Figure 13.- Crash-sequence photographs of -30° (nose-down) test on soil.

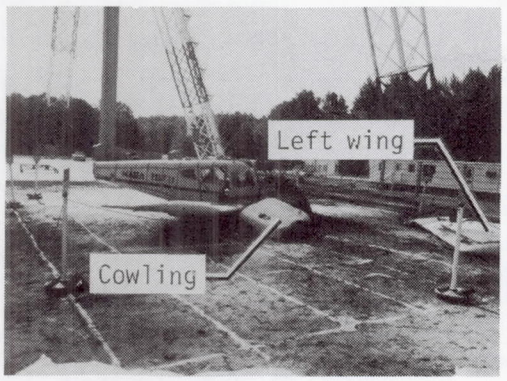

(a) Overall view from front.

(b) Close-up view of front and right side.

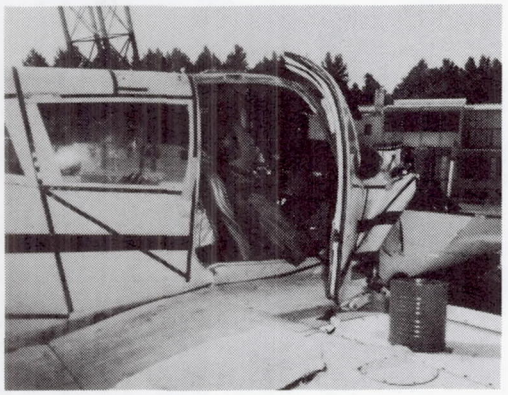

(c) Close-up view of forward cabin and right wing.

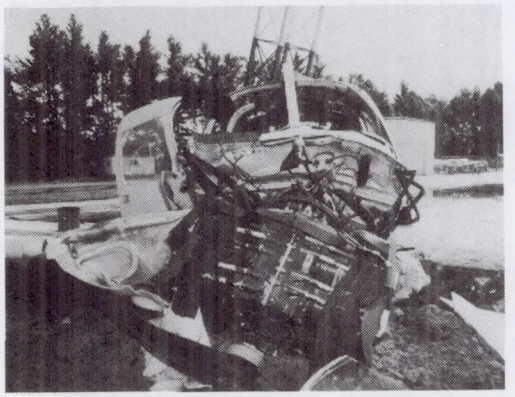

(d) Close-up view of engine compartment and fire wall.

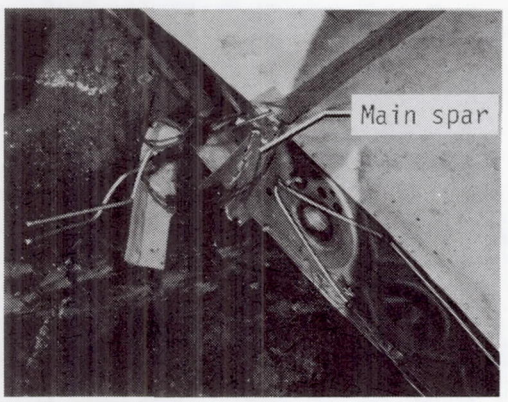

(e) Close-up view of left-wing failure.

(f) Close-up view of crew section.

L-83-104

Figure 14.- Postcrash damage to test specimen in -30° (nose-down) test on soil.

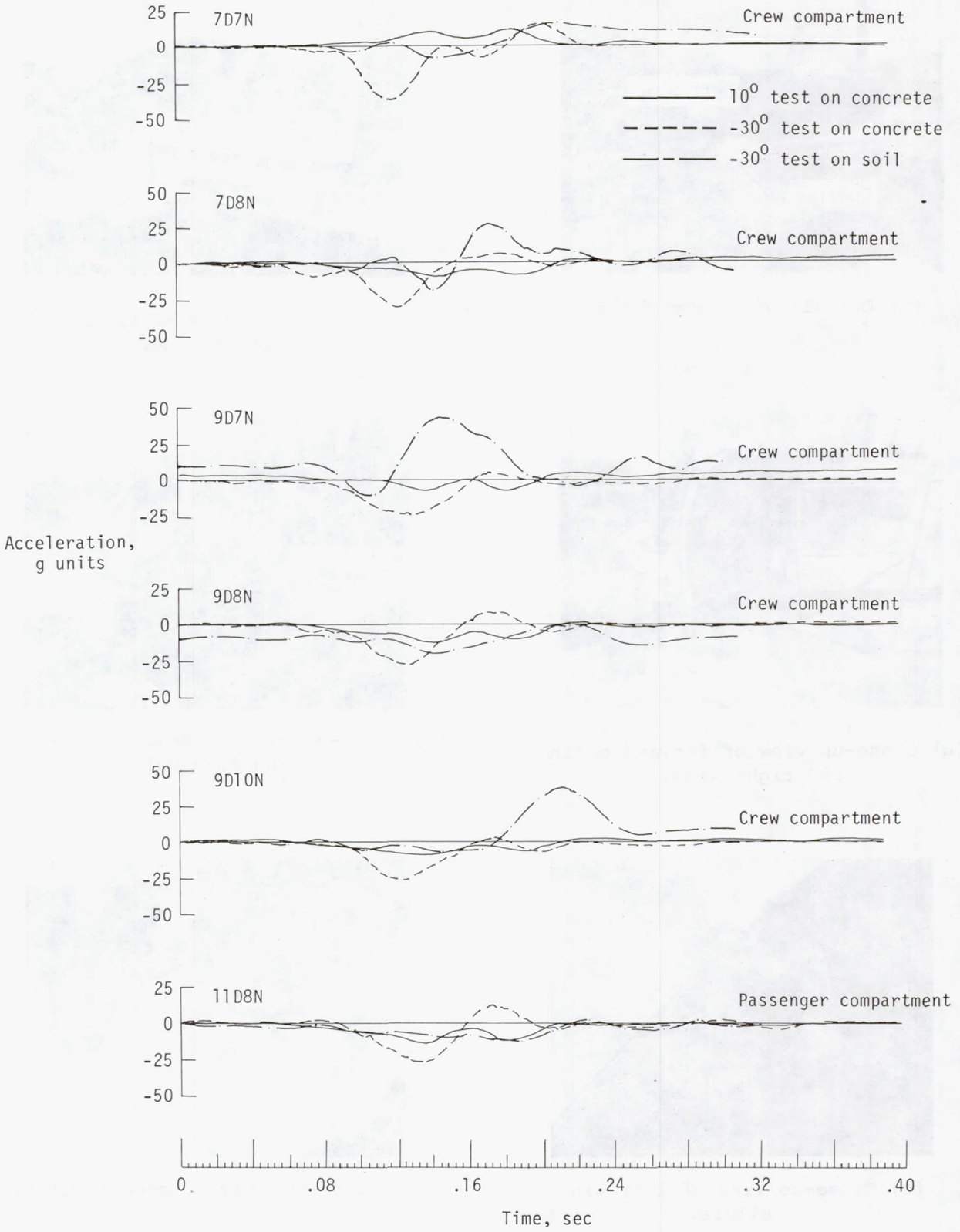

Figure 15.- Normal accelerations on cabin floor in crew and passenger compartments.

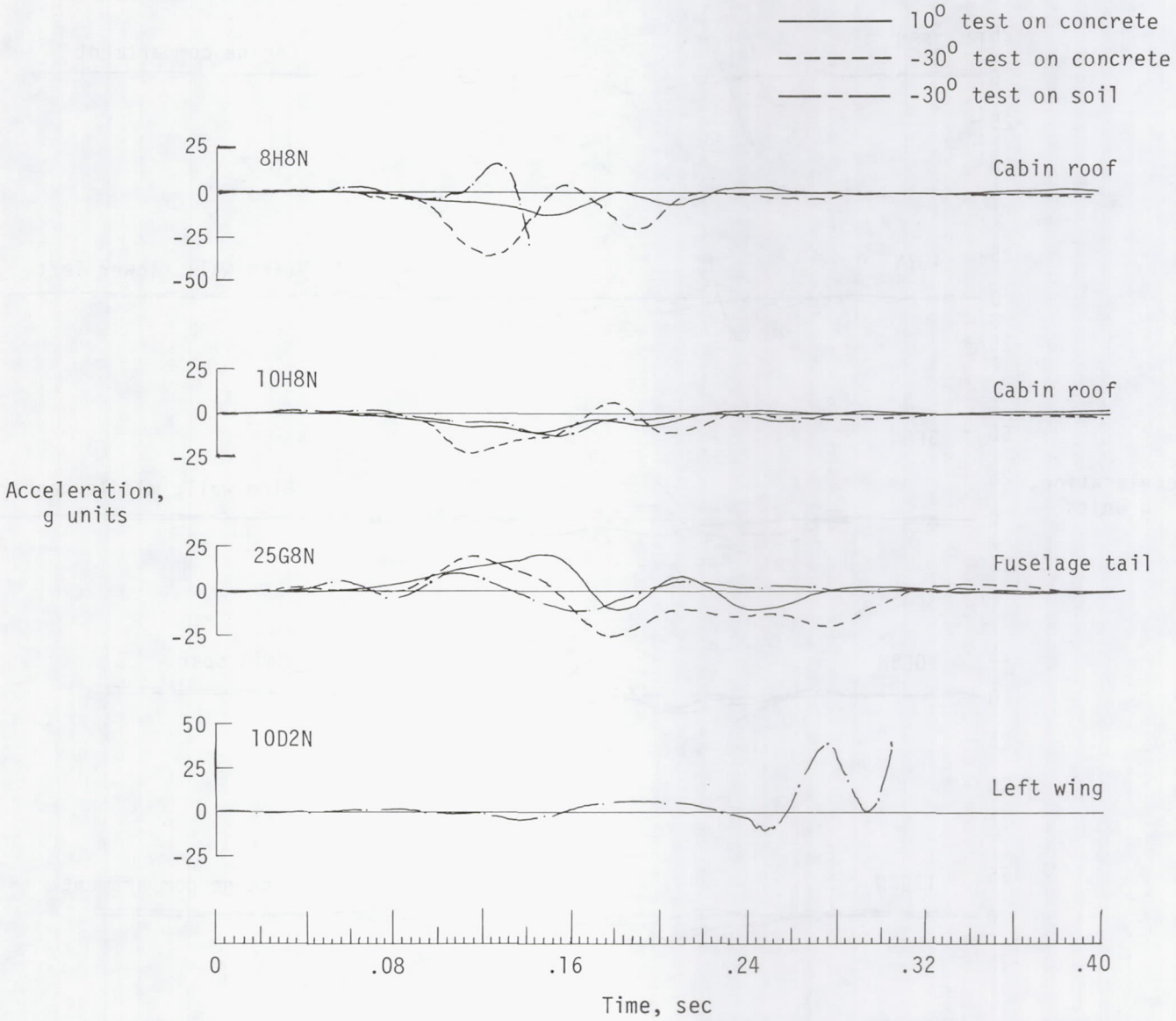

Figure 16.- Normal peak accelerations on cabin roof, fuselage tail, and left wing.

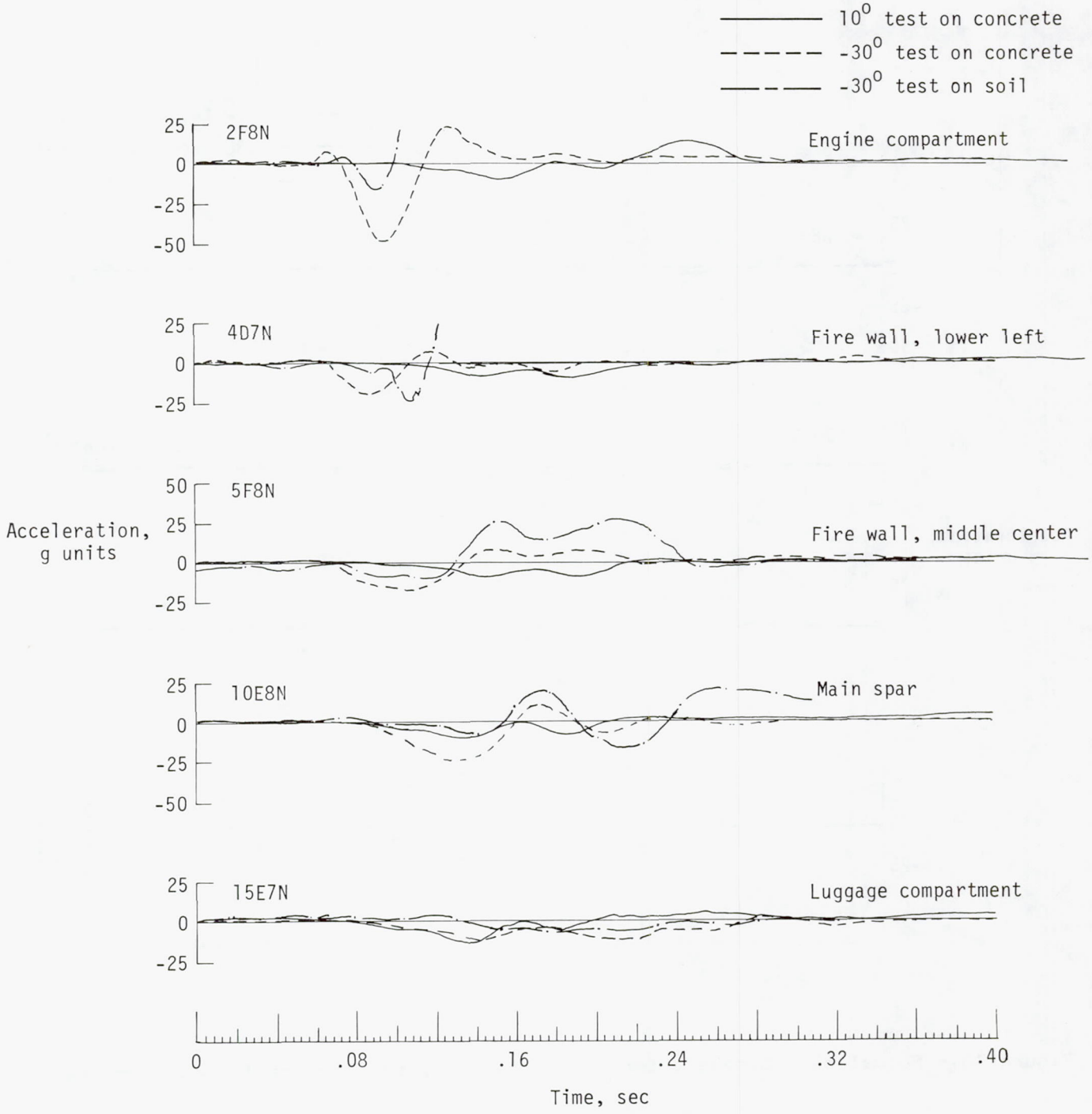

Figure 17.- Normal accelerations in engine compartment and fire wall, main spar, and luggage compartment.

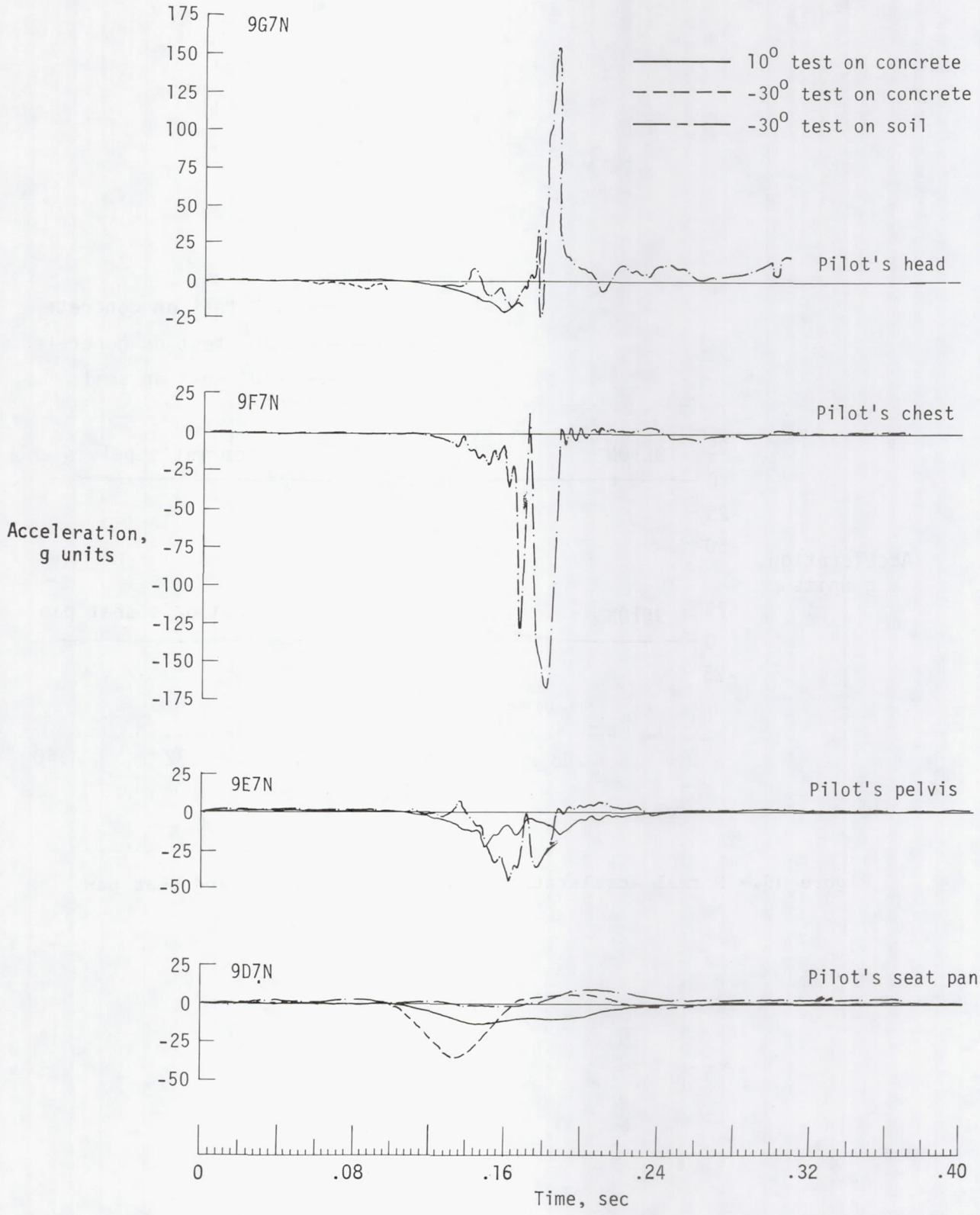

Figure 18.- Normal accelerations in pilot's body and seat pan.

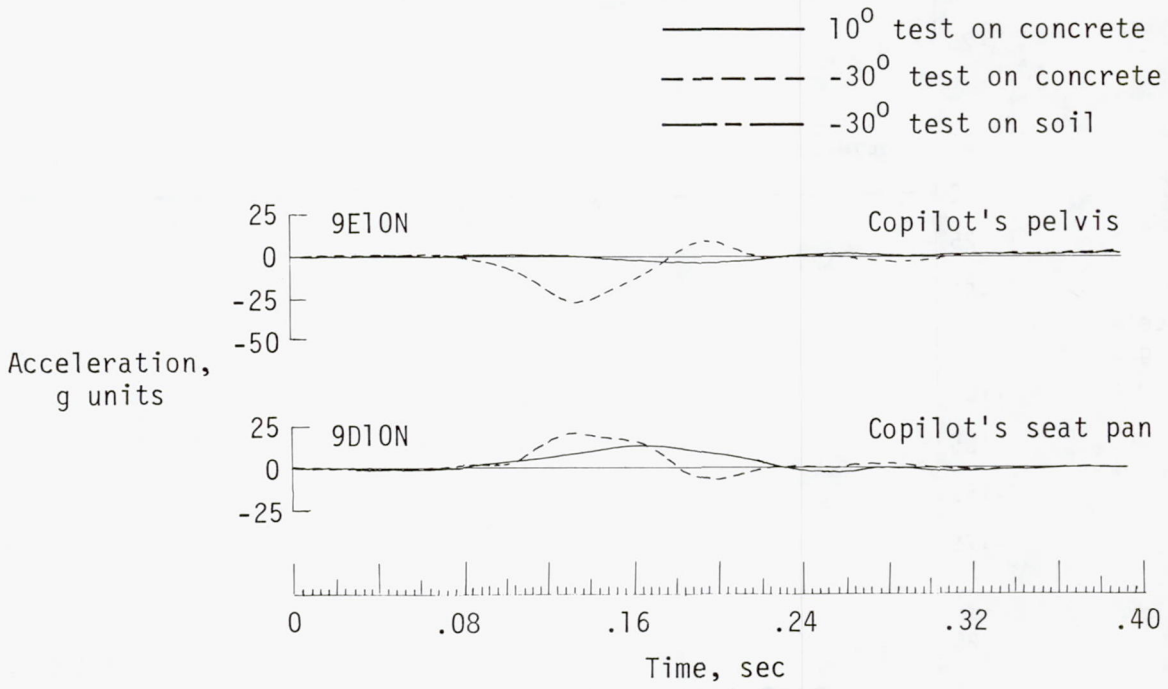

Figure 19.- Normal accelerations in copilot's pelvis and seat pan.

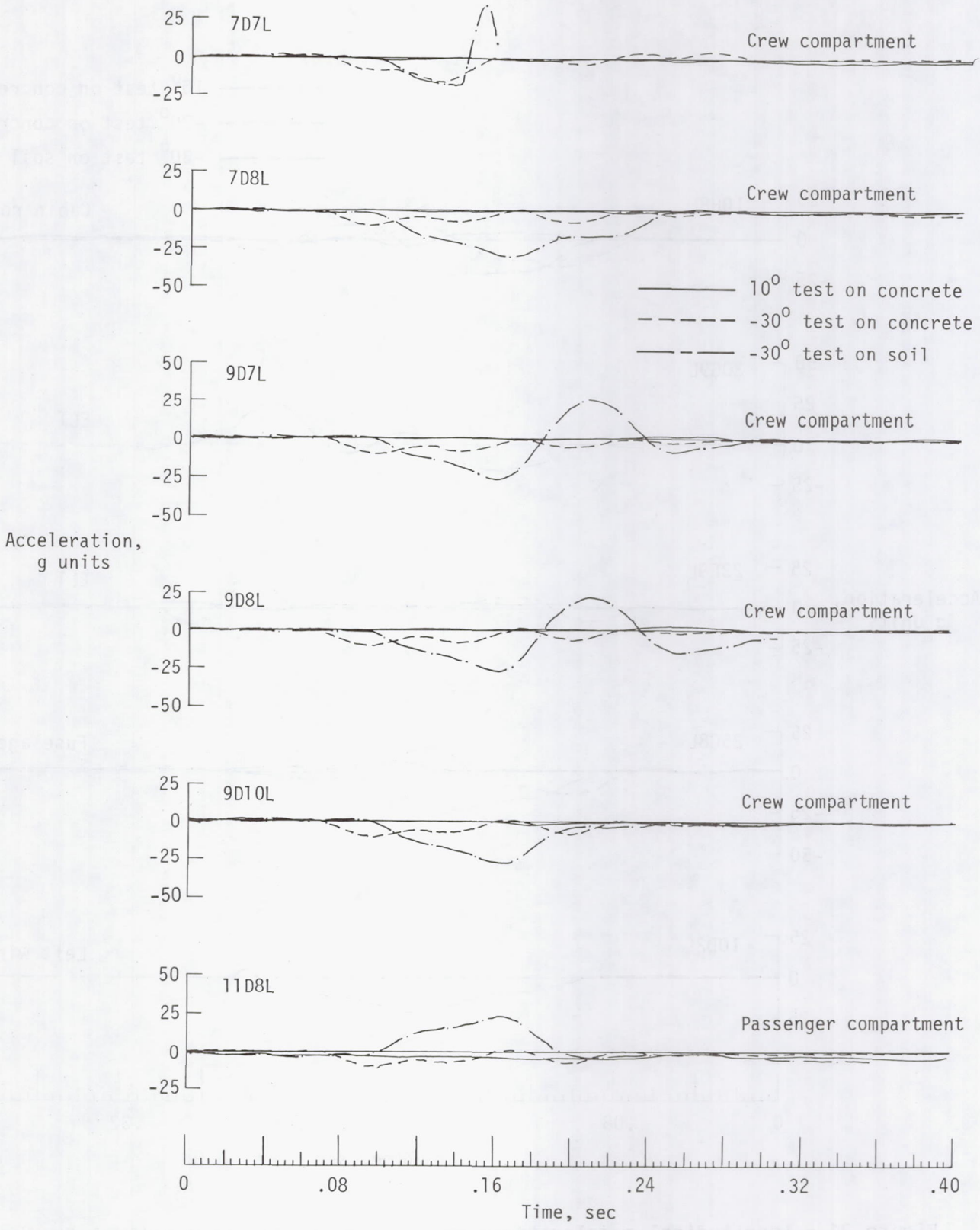

Figure 20.- Longitudinal accelerations on cabin floor in crew and passenger compartments.

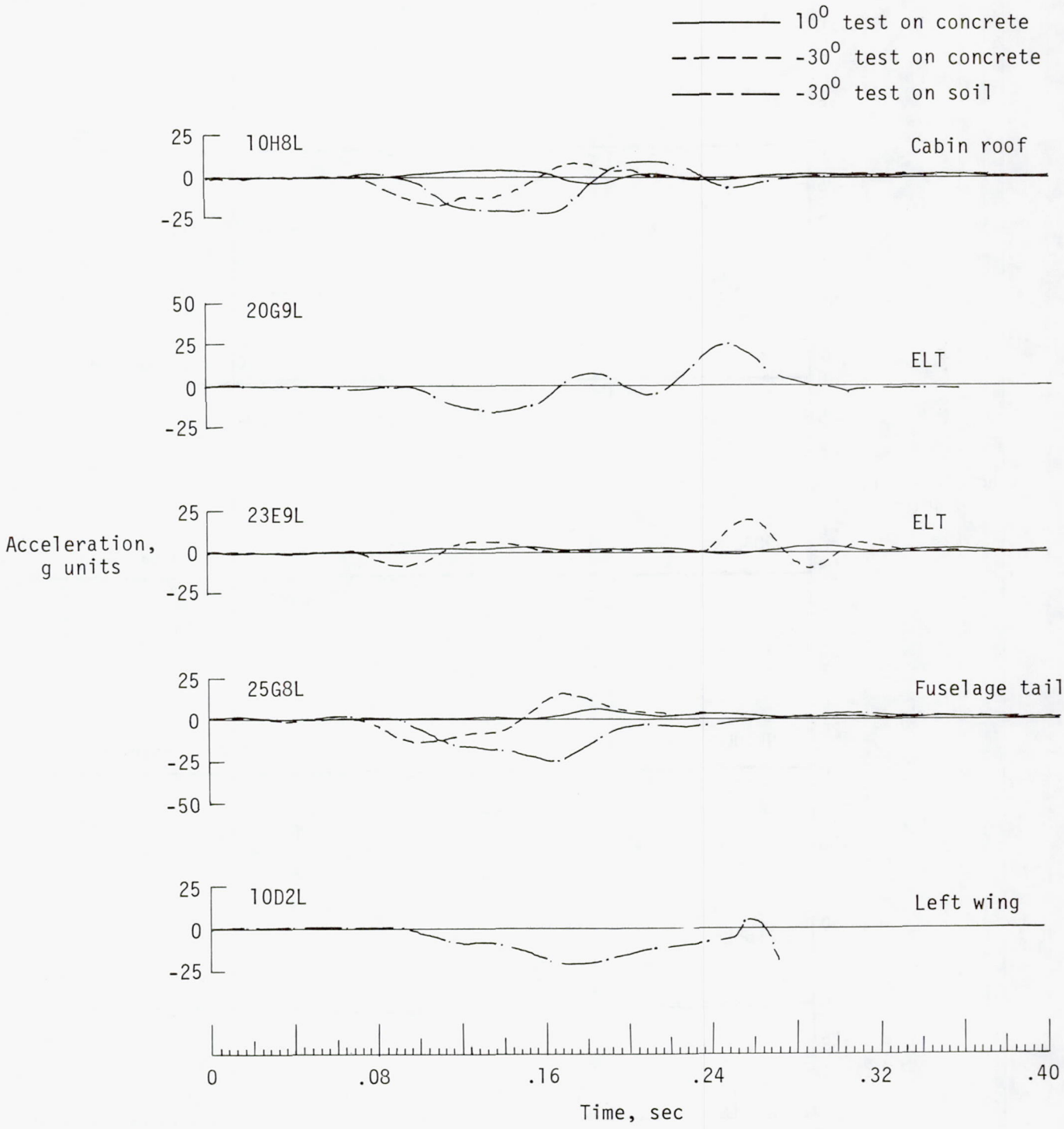

Figure 21.- Longitudinal accelerations on cabin roof, fuselage tail, left wing, and at ELT location.

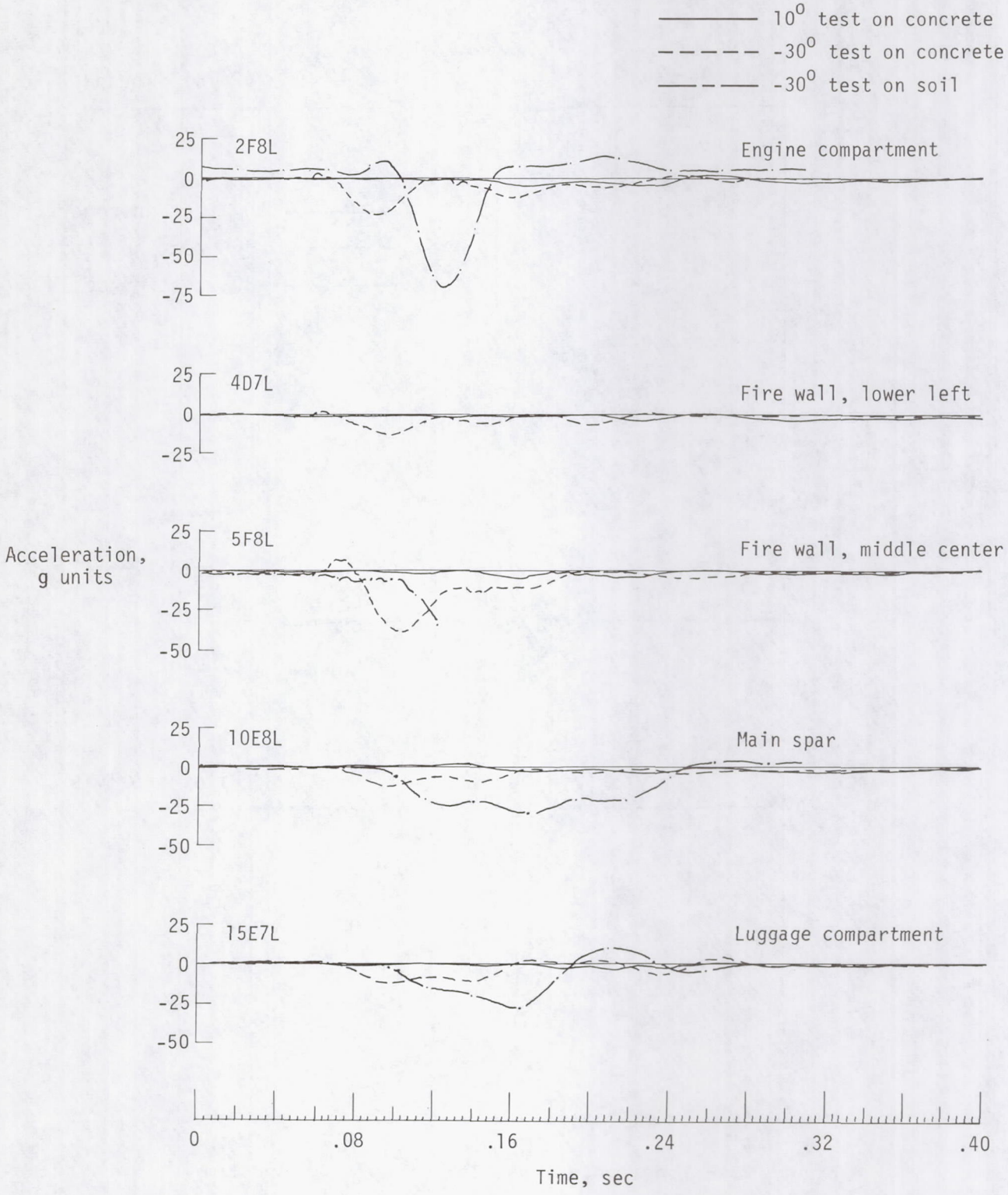

Figure 22.- Longitudinal accelerations in engine compartment and fire wall, main spar, and luggage compartment.

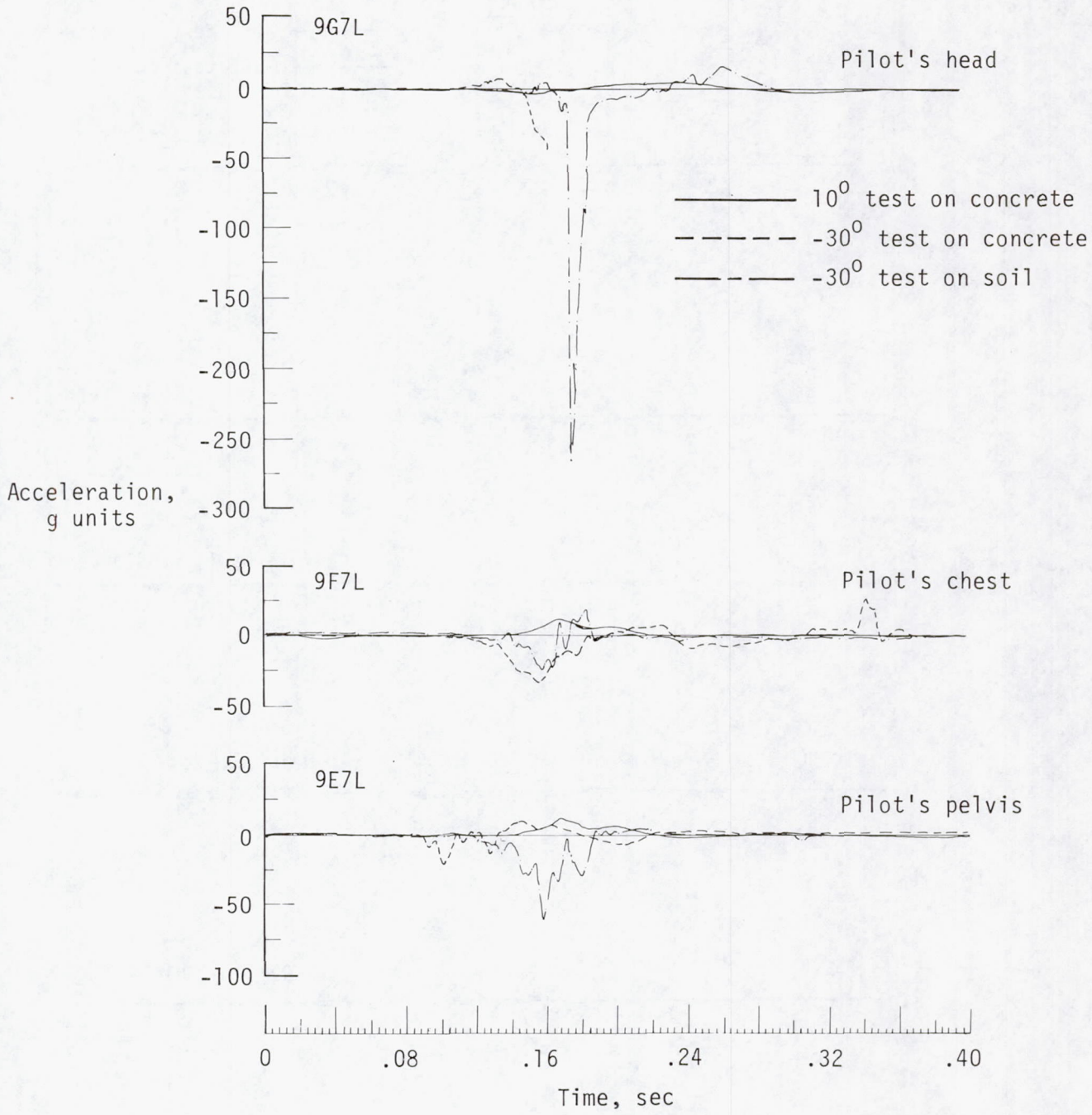

Figure 23.- Longitudinal accelerations in pilot dummy.

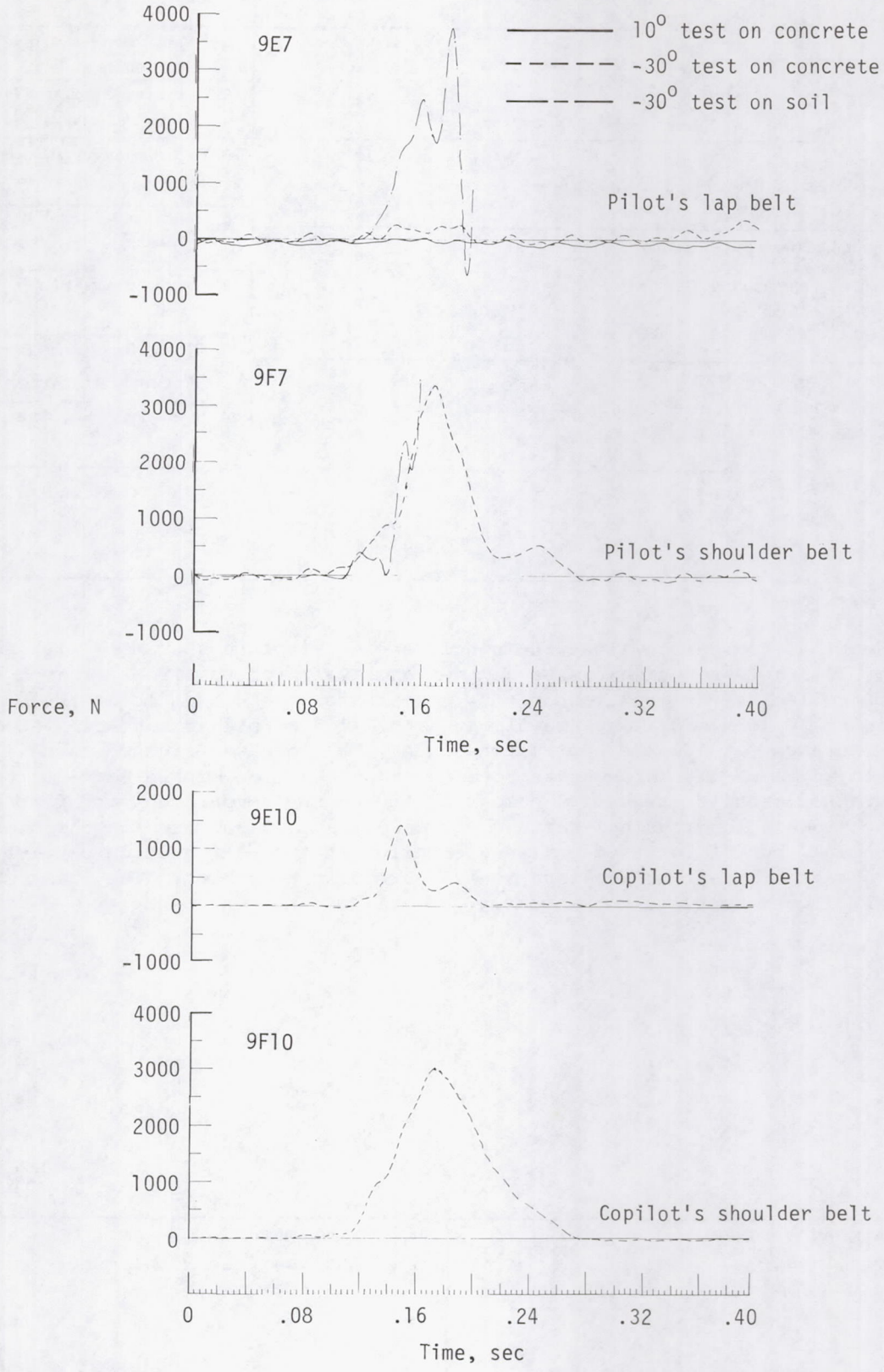

Figure 24.- Tension in restraint-harness system.

1. Report No.	2. Government Accession No.	3. Recipient's Catalog No.
NASA TP-2190		

4. Title and Subtitle	5. Report Date
CRASH TESTS OF THREE IDENTICAL LOW-WING SINGLE-ENGINE AIRPLANES	September 1983
	6. Performing Organization Code 505-33-53-09

7. Author(s)	8. Performing Organization Report No.
Claude B. Castle and Emilio Alfaro-Bou	L-15601
	10. Work Unit No.

9. Performing Organization Name and Address	11. Contract or Grant No.
NASA Langley Research Center Hampton, VA 23665	
	13. Type of Report and Period Covered Technical Paper

12. Sponsoring Agency Name and Address	14. Sponsoring Agency Code
National Aeronautics and Space Administration Washington, DC 20546	

15. Supplementary Notes

16. Abstract

Three identical four-place, low-wing single-engine airplane specimens with nominal masses of 1043 kg were crash-tested at the Langley Impact Dynamics Research Facility under controlled free-flight conditions. The tests were conducted at the same nominal velocity of 25 m/sec along the flight path. Two airplanes were crashed on a concrete surface (at 10° and -30° pitch angles), and one was crashed on soil (at a -30° pitch angle). The three tests revealed that the specimen in the -30° test on soil sustained massive structural damage in the engine compartment and fire wall. Also, the highest longitudinal cabin-floor accelerations occurred in this test. Severe damage, but of lesser magnitude, occurred in the -30° test on concrete. The highest normal cabin-floor accelerations occurred in this test. The least structural damage and lowest accelerations occurred in the 10° test on concrete.

17. Key Words (Suggested by Author(s))	18. Distribution Statement
Crash worthiness Airplane crash tests Crash damage	Unclassified - Unlimited Subject Category 03

19. Security Classif. (of this report)	20. Security Classif. (of this page)	21. No. of Pages	22. Price
Unclassified	Unclassified	38	A03

For sale by the National Technical Information Service, Springfield, Virginia 22161

NASA-Langley, 1983